Multi-Objective Optimization for Spectrum and Energy Efficiency Tradeoff in IRS-Assisted CRNs with NOMA

Yuhang Wu, Fuhui Zhou, *Senior Member, IEEE*,
Wei Wu, *Member, IEEE*, Qihui Wu, *Senior Member, IEEE*,
Rose Qingyang Hu, *Fellow, IEEE*, Kai Kit Wong, *Fellow, IEEE*

Abstract

Non-orthogonal multiple access (NOMA) is a promising candidate for the sixth generation wireless communication networks due to its high spectrum efficiency (SE), energy efficiency (EE), and massive connectivity. It can be applied in cognitive radio networks (CRNs) to further improve SE and user connectivity. However, the interference caused by spectrum sharing and the utilization of non-orthogonal resources should be controlled, which limits the achievable performance. In order to tackle this issue, intelligent reflecting surface (IRS) is exploited in a downlink multiple-input-single-output (MISO) CRNs with NOMA. Since the tradeoff between SE and EE is of crucial importance, a multi-objective optimization (MOO) framework is formulated under both the perfect and imperfect channel state information (CSI). An iterative block coordinate descent (BCD)-based algorithm is exploited to optimize the beamforming design and IRS reflection coefficients iteratively under the perfect CSI case. A safe approximation and the $\mathcal{S}$-procedure are used to address the non-convexity infinite inequality constraints of the problem under the imperfect CSI case. Simulation results demonstrate that the proposed scheme can achieve a better

Y. Wu, F. Zhou, and Q. Wu are with the School of Electronic Engineering, Nanjing University of Astronautics and Aeronautics, P. R. China, 330031 (e-mail: may_wyh@nuaa.edu.cn; zhoufuhui@nuaa.edu.cn; wuqihui2014@sina.com).

W. Wu is with the College of Communication and Information Engineering, Nanjing University of Posts and Telecommunications, Nanjing 210003, China (e-mail: weiwu@njupt.edu.cn).

R. Q. Hu is with the Department of Electrical and Computer Engineering, Utah State University, Logan, UT 84322 USA (e-mail: rose.hu@usu.edu).

K.-K. Wong is with the Department of Electronic and Electrical Engineering, University College London, London, WC1E 6BT, UK (e-mail: kaikit.wong@ucl.ac.uk).

The research reported in this article was supported by the Natural Science Foundation of China (61631015, 61501356, 61661028, and 61561034), and the National key scientific and technological innovation team plan (2016KCT-01).

balance between SE and EE than baseline schemes. Moreover, it is shown that both the SE and EE of the proposed algorithm under the imperfect CSI can still be significantly improved due to the exploitation of IRS.

Index Terms

Intelligent reflecting surface, cognitive radio, non-orthogonal multiple access, spectral efficiency, energy efficiency, multi-objective optimization, block coordinate descent, robust design.

I. Introduction

THE fifth generation (5G) wireless communication networks are commercially applied and continuously deployed worldwide. Although they have made great breakthrough advancements in wireless communication techniques, several limitations are gradually appeared along with the unprecedented proliferation of user connectivity, the emergence of diverse real-time and ultra-wideband communication services, and the urgent requirement of green operations [1], [2]. Thus, it is imperative and important to develop the sixth generation (6G) wireless communication networks. Non-orthogonal multiple access (NOMA) has been envisioned as a candidate multiple access scheme for the 6G wireless communication networks since it can improve both spectrum efficiency (SE) and energy efficiency (EE), and increase user connectivity [3]. The main difference between NOMA and orthogonal multiple access (OMA) is that NOMA exploits non-orthogonal resources, such as the power, to distinguish the signal of different users [4]. The successive interference cancellation (SIC) technique is adopted at receivers for decoding the desired information while mitigating the mutual interference caused by signal superimposing [5].

Due to the advantages of NOMA, the application of NOMA into cognitive radio networks (CRNs) can further alleviate the spectrum scarcity problem, and enhance user connectivity [6]. In CRNs with NOMA, the secondary users (SUs) are allowed to share the spectrum bands of the primary users (PUs) in the power domain, given that the interference caused by SUs does not exceed the tolerance threshold of the PUs [7]. Recently, many researchers from both academic and industry have focused on CRNs with NOMA and have made great achievements [8]-[10].

In CRNs with NOMA, since the quality of service of PUs should be guaranteed, the interference caused by spectrum sharing and the utilization of non-orthogonal resources should be limited. Thus, the transmit power of the secondary base station (SBS) cannot be high, which limits the performance of SUs. Recently, intelligent reflecting surface (IRS) is viewed as revolutionary technology pertaining to 6G due to its potential of simultaneously improving EE and SE [11]. In particular, IRS is a planer

metasurface comprising a large number of passive reflecting elements. By properly designing the reflecting coefficients of IRS, the reflected signals can be combined at the receivers constructively to improve the desired signal power and mitigate the interference at the same time, thereby improving system SE without further energy consumption [12]-[15]. It is envisioned that IRS can be exploited to simultaneously improve the performance of SUs and decrease the interference caused to the PUs in CRNs with NOMA. Thus, it is of great interest to investigate the IRS-assisted CRNs with NOMA. In order to explore the potential performance improvement obtained by exploiting IRS in CRNs with NOMA in terms of SE and EE and address the tradeoff between SE and EE, a multiple-objective optimization (MOO) framework is formulated in downlink multiple-input-single-output (MISO) IRS-assisted CRNs with NOMA. The related works and the motivations of our work are summarized as follows.

A. Related Work and Motivation

Resource allocation problems have been extensively investigated in the conventional NOMA networks [16]-[18] and also in CRNs with NOMA [19]-[24]. Moreover, the benefits of IRS for enhancing SE and EE have been demonstrated in NOMA systems [25]-[33]. These related works are presented as follows.

In the conventional NOMA networks, the energy-efficient resource allocation design was investigated in [16]. Specifically, a sub-optimal user scheduling and power allocation design was proposed under the perfect channel state information (CSI). It was showed that NOMA can achieve higher EE than OMA. Based on the work in [16], the authors extended the maximization of EE into the system with NOMA under the imperfect CSI. An iterative algorithm was proposed for maximizing the system EE by optimizing the user scheduling and power allocation. Different from the works in [16] and [17], the authors in [18] focused on maximizing SE of the systems with NOMA, where a minorization-maximization algorithm was proposed. It was shown that NOMA is also superior to OMA in terms of SE.

In order to alleviate the spectrum scarcity problem and enhance user connectivity, resource allocation problems have also been studied in CRNs with NOMA. The authors in [19] studied a full-duplex CRNs with NOMA, where the simultaneous wireless information and power transmission was considered. An iterative algorithm was proposed to maximizing the throughput of the secondary networks. The results showed that the achievable throughput of CRNs with NOMA is superior to that of CRNs with OMA. The authors of [20] studied the throughput maximization problem by optimizing the power allocation and time-sharing coefficient in CRNs with NOMA. In contrast to the works in [19] and [20], the authors of [21] aimed to improve the SE of the primary networks. The power allocation was optimized for maximizing the sum-rate. The results showed that the SE of PUs achieved in CRNs with NOMA outperforms that obtained in CRNs with NOMA.

In contrast to the works in [19]-[21], the works in [22]-[24] optimized the EE of CRNs with NOMA. An efficient algorithm was proposed in CRNs with NOMA by using the sequential convex approximation method to enhance EE in [22]. It was shown that the EE achieved in CRNs with NOMA is higher than that obtained in CRNs with OMA. In [23], the authors investigated the minimization of the transmit power in MISO CRNs with NOMA relying on simultaneous wireless information and power transfer (SWIPT) under a practical non-linear EH model. The bounded CSI error model was considered to describe the channel uncertainty. The author extended the work in [23] by considering both bounded and the Gaussian CSI error model in [24]. The harvested energy was maximized by jointly designing the robust beamforming and power splitting control.

Although NOMA can further improve the SE and user connectivity of CRNs, the complexity of the receiver and interference caused by using non-orthognal resource increase with the number of NOMA users, which results in unpractical design and even poor performance. In order to tackle the inherent disadvantages of NOMA, the promising IRS technique has been exploited in NOMA and resource allocation problems were studied in [25]-[33]. In [25], an IRS-assisted system with NOMA was considered. A joint optimization of the beamforming and reflection coefficient was investigated. It was shown that the SE of the system with NOMA can be further improved with the exploitation of IRS. In [26], the ideal and non-ideal IRS assumptions were considered in the sum rate maximization by jointly optimizing the active and passive beamforming vectors subject to SIC decoding rate conditions and IRS reflection coefficients constraints. The work in [27] is the expansion of [26] in robust transmission for two-users IRS-assisted systems with NOMA, in which the multi-antenna eavesdroppers under the imperfect CSI were considered.

In contrast to the conventional systems with NOMA, the SIC decoding order of IRS-assisted systems with NOMA highly depends on the adjustment of the passive elements of IRS. Therefore, a novel SIC decoding order searching algorithm was proposed in the IRS-assisted system with NOMA via maximizing the combined channel power gains of each user in [28]. After obtaining the optimal decoding order, the joint power allocation and phase shift optimization problems were tackled by using the alternative optimization (AO) algorithm and semidefinite relaxation (SDR) method. Moreover, the authors expanded the work in [28] into multi-antenna scenarios, and the block coordinate descent (BCD) and SDR were utilized to solve the maximization of target signal-interference-noise-ratio [29]. The authors in [30] proposed a joint optimization problem of power allocation, reflection matrix, and decoding order in multi-cell IRS-assisted systems with NOMA, where the decoding order and IRS reflection matrix were jointly designed for improving SE.

The works in [28]-[30] demonstrated the improvement of SE in IRS-assisted systems with NOMA, while EE was not considered. Thus, the work in [31] focused on the energy-efficient design of IRS-assisted systems with NOMA, in which the system EE was maximized by alternatively optimizing the transmit beamforming and the IRS reflection coefficients. It was showed that the proposed resource allocation scheme of IRS-assisted systems with NOMA has higher EE than that achieved by the IRS-assisted systems with OMA. However, the work in [31] did not consider the direct links among the base station and users. Therefore, the authors in [32] considered the direct link in an IRS-assisted system with NOMA. An AO framework was adopted, while a novel difference-of-convex (DC) programming algorithm was developed. The authors in [33] studied an IRS-assisted system with NOMA, where the EE maximization problem was investigated with considering the data requirements of users. It was demonstrated that the application of IRS in the system with NOMA is capable of achieving higher EE than IRS-assisted systems with OMA.

It is envisioned that IRS can significantly benefit for CRNs with NOMA. Although resource allocation problems have been well studied in NOMA systems [16]-[18], CRNs with NOMA [19]-[24] and IRS-assisted NOMA systems [25]-[33], to the best authors' knowledge, there are no investigations focused on resource allocation schemes in the IRS-assisted CRNs with NOMA. Moreover, resource allocation schemes proposed in the works mentioned above are not suitable for IRS-assisted CRNs with NOMA since the success of SIC at users not only depends on the direct links but also the reflecting links constructed by IRS. Furthermore, the resource allocation schemes for IRS-assisted CRNs with OMA proposed in [34]-[36] are inappropriate to IRS-assisted CRNs with NOMA since the non-orthogonal resources are utilized. Thus, in order to further improve both SE and EE and provide massive connectivity, it is of great importance to study the resource allocation problems in IRS-assisted MISO CRNs with NOMA.

B. Contributions

To the authors' best knowledge, few studies have been conducted for the joint active and passive beamforming design in IRS-assisted MISO CRNs with NOMA under both the perfect and imperfect CSI. Moreover, since SE and EE are essential performance metrics, the competition between them requires intensive study [37]. However, the tradeoff between SE and EE has not been well studied in IRS-assisted CRNs with NOMA. Unfortunately, how to design an appropriate resource allocation for simultaneously enhancing both SE and EE under the constraints on the interference and the successful implementation of SIC presents a fundamental challenge, especially for the imperfect CSI case. Moreover, couples exist among different variables, such as the beamforming and the phase shifts of IRS, which makes the problems non-convex and challenging. Thus, in order to optimize the resource allocation design for comprehensively

investigating the tradeoff between SE and EE, it is vital to study the active beamforming and the IRS reflection coefficients design in IRS-assisted CRNs with NOMA. The main contributions are summarized as follows.

- A MOO framework is formulated in IRS-assisted downlink MISO CRNs with NOMA to simultaneously optimize SE and EE while addressing the tradeoff between them. The formulated problems are non-convex and intractable. A low-complexity decoding order design is first proposed to obtain the SIC decoding orders of SUs. Moreover, the ϵ-constraint method is adopted to transform the MOO problems (MOOPs) into single-objective optimization problems (SOOPs). Furthermore, a BCD-based iterative algorithm is proposed, where the original problem is decomposed into two sub-optimization problems to design the optimal beamforming vectors and the phase shift iteratively.
- Considering that the perfect CSI cannot be obtained since the cooperation between PUs and SUs may not exist in practice, the MOOP is studied under the imperfect CSI case. The worst-case is considered to provide a robust resource allocation algorithm under the bounded channel error model. Moreover, a safe approximation is applied to transform the intractable non-convex maximum interference constraint into a convex constraint. Furthermore, the $\mathcal{S}$-procedure method is capitalized to deal with the channel uncertainty for designing the robust resource allocation to maximize SE and EE simultaneously. The BCD-based iterative algorithm under the imperfect CSI case is also used to make the challenging optimization problem more tractable.
- Simulation results demonstrate that the exploitation of IRS in CRNs with NOMA can achieve a better balance between SE and EE, even under the imperfect CSI case. Moreover, it is shown that our proposed resource allocation schemes can simultaneously improve EE and SE compared to the baseline schemes. Furthermore, the convergence and efficiency of our proposed algorithms are also demonstrated.

C. Organization and Notations

The remainder of this paper is organized as follows. Section II introduces the system model and formulates the MOOP in order to investigate the tradeoff between SE and EE. Section III presents a low complexity decoding order optimization problem and its solution. In Section IV, the MOOP under the perfect CSI is studied. In Section V, the MOOP is investigated under the imperfect CSI. Simulation results are presented in Section VI. Finally, this paper is concluded in Section VII.

Notations: Vectors and matrices are represented by boldface lower case letters and boldface capital letters, respectively. The $\mathbb{R}^{N\times M}$ and $\mathbb{C}^{N\times M}$ denote the space of $N\times M$ real-valued and complex-valued matrices, respectively. $\mathbf{I}_N$ represents the $N\times N$ identity matrix. The set of all N-dimensional complex

Hermitian matrices is denoted by $\mathbb{H}^N$. The trace, rank and the (i,i)-entry of a matrix $\mathbf{A}$ are denoted respectively by $\mathrm{Tr}(\mathbf{A})$, $\mathrm{Rank}(\mathbf{A})$ and $[\mathbf{A}]_{i,i}$. $\mathbf{A}^T$, $\mathbf{A}^*$, and $\mathbf{A}^H$ denote the transpose, the conjugate, and the Hermitian (conjugate) transpose of matrix $\mathbf{A}$. $\mathbf{A} \succeq$ represents that $\mathbf{A}$ is a Hermitian positive semidefinite matrix. $|\cdot|$ and $\|\cdot\|$ represent the absolute value of a complex scalar and the Euclidean norm of a vector, respectively. $\mathrm{diag}(\mathbf{x})$ denotes an $N \times N$ diagonal matrix with main diagonal elements $x_1, \ldots, x_N$. $\mathbf{x} \sim \mathcal{CN}(\boldsymbol{\mu}, \boldsymbol{\Sigma})$ means that $\mathbf{x}$ is a random vector, which follows the distribution of complex Gaussian with mean $\boldsymbol{\mu}$ and variance $\boldsymbol{\Sigma}$. $\nabla_{\mathbf{x}} f(\mathbf{x})$ denotes the gradient vector of function $f(\mathbf{x})$ with respect to $\mathbf{x}$. The optimal value of optimization variable $\mathbf{x}$ is denoted by $\mathbf{x}^{\ddagger}$.

II. System Model

A. System Model

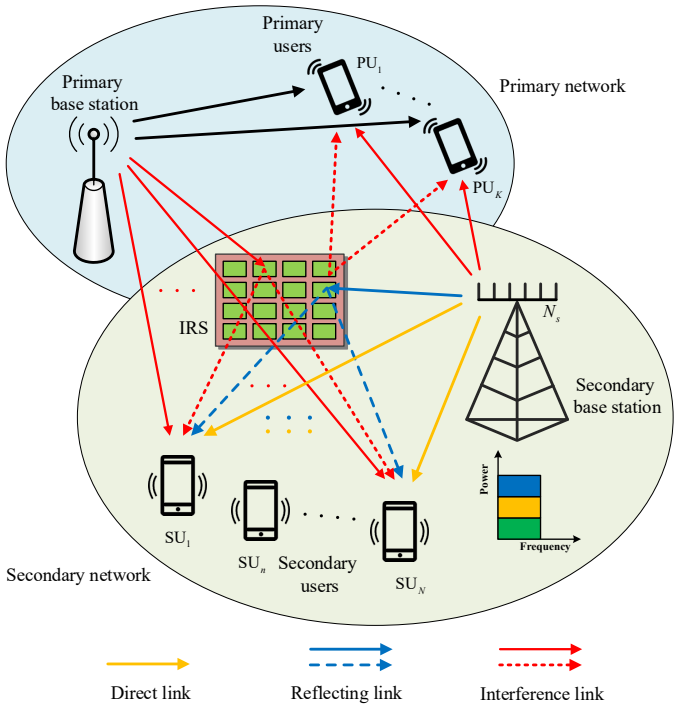

Fig. 1. The system model.

As illustrated in Fig. 1, an IRS-assisted downlink CRN with NOMA is considered, which consists of a licensed primary network and an unlicensed secondary network. Specifically, the primary network comprises one primary base station (PBS) and K PUs, while the secondary network contains one SBS and N SUs. Let $\mathcal{K} = \{1, 2, \ldots, K\}$ and $\mathcal{N} = \{1, 2, \ldots, N\}$ denote the set of PUs and SUs, respectively. The SBS is equipped with N_s antennas, while the PBS, K PUs and N SUs are equipped with a single antenna.

Besides, an IRS with M passive reflecting elements, denoted by $\mathcal{M} = \{1, 2, \ldots, M\}$, is deployed in the secondary network to enhance the transmission from the SBS to SUs. The diagonal phase shift matrix of IRS is denoted by $\mathbf{\Theta} = \mathrm{diag}\{\beta_1 e^{j\theta_1}, \beta_2 e^{j\theta_2}, \ldots, \beta_M e^{j\theta_M}\}$, where $\beta_m \in [0, 1]$ and $\theta_m \in [0, 2\pi]$ denote the amplitude and phase shift of the mth passive reflecting elements, respectively.

In order to realize NOMA, the superposition coding is employed at the SBS. The data flow for each SU is assigned with a dedicated beamforming vector. Then, the SBS broadcasts the superimposed signal to all SUs. Thus, the transmitted superposition of K data flows from the SBS to the SUs can be given as

$$\boldsymbol{x} = \sum_{n=1}^{N} \mathbf{w}_n x_n, \tag{1}$$

where $x_n \sim \mathcal{CN}(0, 1)$ and $\mathbf{w}_n \in \mathbb{C}^{N_s \times 1}$ are the data flow intended to the nth SU and the corresponding beamforming vector, respectively.

The received signals at the kth PU and the nth SU are respectively given by,

$$y_k^P = \sqrt{p_k^P} s_k + (\mathbf{h}_{k,I}^H + \mathbf{f}_{k,R}^H \mathbf{\Theta} \mathbf{g}_{SI}) \boldsymbol{x} + n_k, \tag{2a}$$

$$y_n^S = \underbrace{\left(\mathbf{g}_{n,D}^H + \mathbf{g}_{n,R}^H \mathbf{\Theta} \mathbf{g}_{SI}\right) \mathbf{w}_n x_n}_{\text{desired signal}} + \underbrace{\sum_{i \in \mathcal{N}, i \neq n}^{N} \left(\mathbf{g}_{n,D}^H + \boldsymbol{g}_{n,R}^H \mathbf{\Theta} \mathbf{g}_{SI}\right) \mathbf{w}_i x_i}_{\text{multiuser interference}}$$

$$+ \underbrace{\left(f_{n,D}^P + \mathbf{g}_{n,R}^H \mathbf{\Theta} \mathbf{f}_{PI}\right) \sum_{k \in K} \sqrt{p_k^P} s_k}_{\text{interference from the primary network}} + n_n, \tag{2b}$$

where $\mathbf{h}_{k,I} \in \mathbb{C}^{N_s \times 1}$ and $\mathbf{f}_{k,R} \in \mathbb{C}^{M \times 1}$ denote the channel vector between the SBS and the kth PU and the channel vector between the IRS and the kth PU, respectively. The channel between the SBS and the nth SU is denoted by $\mathbf{g}_{n,D} \in \mathbb{C}^{N_s \times 1}$. $\mathbf{g}_{n,R} \in \mathbb{C}^{M \times 1}$ denotes the reflecting channel between the IRS and the nth SU. The channel between the PBS and the nth SU is denoted by $f_{n,D}^P$. The baseband equivalent channel between the SBS and the IRS and the channel between the PBS and the IRS are modeled as $\mathbf{g}_{SI} \in \mathbb{C}^{M \times N_s}$ and $\mathbf{f}_{PI} \in \mathbb{C}^{M \times 1}$, respectively. The transmit power from the PBS to the kth PU is denoted by $p_k^P \in \mathbb{R}$, and the information symbol for the kth PU transmitted by PBS is represented by $s_k \in \mathbb{C}$. $n_k \sim \mathcal{CN}(0, \sigma^2)$ and $n_n \sim \mathcal{CN}(0, \sigma^2)$ are the additive white Gaussian noises (AWGNs) at the kth PU and the nth SU, respectively.

According to the NOMA principle, SIC is employed at the SUs to remove the co-channel interference. An optimal SIC decoding order plays a vital role in systems with NOMA, which is determined by the channel power gains. Specifically, the SU with a higher channel power gain can decode the signal of the

SU with a weaker channel power gain, and extracts them from the received signal. However, in IRS-assisted CRNs with NOMA, the combined channel power gains are influenced by changing the phase shift matrix of IRS, i.e., $\mathbf{\Theta}$. Thus, the decoding order of the SUs is required to be designed based on the combined channel power gain, which will be presented in Section III. Let $\pi(n)$ denote the decoding order for the nth SU. Then, $\pi(n) = n$ represents that the nth SU is the nth signal to be decoded, while the signal of the ith SU with $\pi(j) > \pi(n)$ is treated as interference. The signal of the mth SU with $\pi(m) < \pi(n)$ is previously decoded at the kth SU and is removed from the received signal [26]. Therefore, the achievable signal-to-interference-plus-noise ratio (SINR) at the nth SU to decode its own signal can be written as

$$\text{SINR}_{n\to n} = \frac{\left|\left(\boldsymbol{g}_{n,D}^H + \boldsymbol{g}_{n,R}^H \mathbf{\Theta} \boldsymbol{g}_{SI}\right)\mathbf{w}_n\right|^2}{\sum\limits_{\pi(i)>\pi(n)}^{N}\left|\left(\boldsymbol{g}_{n,D}^H + \boldsymbol{g}_{n,R}^H \mathbf{\Theta} \boldsymbol{g}_{SI}\right)\mathbf{w}_i\right|^2 + \sum\limits_{k=1}^{K}\left|f_{n,D}^P + \boldsymbol{g}_{n,R}^H \mathbf{\Theta} \boldsymbol{f}_{PI}\right|^2 p_k^P + n_n}. \tag{3}$$

The corresponding achievable rate at the nth SU to decode its own signal is represented as $R_{n\to n} = \log_2(1 + \text{SINR}_{n\to n})$.

In this paper, $\pi(j) > \pi(k)$ means that the jth SU is able to decode the signal of the kth SU. The corresponding SINR for the jth SU decoding the signal intended to the kth SU can be expressed as

$$\text{SINR}_{n\to j} = \frac{\left|\left(\mathbf{g}_{j,D}^H + \mathbf{g}_{j,R}^H \mathbf{\Theta} \mathbf{g}_{SI}\right)\mathbf{w}_n\right|^2}{\sum\limits_{\pi(i)>\pi(n)}^{N}\left|\left(\mathbf{g}_{j,D}^H + \boldsymbol{g}_{j,R}^H \mathbf{\Theta} \mathbf{g}_{SI}\right)\mathbf{w}_i\right|^2 + \sum\limits_{k=1}^{K}\left|f_{j,D}^P + \mathbf{g}_{j,R}^H \mathbf{\Theta} \mathbf{f}_{PI}\right|^2 p_k^P + n_j}. \tag{4}$$

Accordingly, the achievable rate of the jth SU to decode the signal of the kth SU is $R_{n\to j} = \log_2(1 + \text{SINR}_{n\to j})$.

In order to guarantee that the jth user can decode the kth user's signal successfully under the decoding order $\pi(j) > \pi(k)$, the achievable rate at the jth SU to decode the kth SU's signal should be greater than the achievable rate of the kth SU decoding its own signal. That is, the SIC decoding condition $R_{n\to j} \geq R_{n\to n}$ needs to be guaranteed.

Moreover, the power allocated to each SU should be inversely proportional to its channel strength based on the given decoding orders, which can avoid the case that the high decoding order SU uses most of the wireless resources [28]. Therefore, the following condition should be satisfied

$$\left|\left(\mathbf{g}_{n,D}^H + \mathbf{g}_{n,R}^H \mathbf{\Theta} \mathbf{g}_{SI}\right)\mathbf{w}_{\pi(i)}\right|^2 \leq \left|\left(\mathbf{g}_{n,D}^H + \mathbf{g}_{n,R}^H \mathbf{\Theta} \mathbf{g}_{SI}\right)\mathbf{w}_{\pi(j)}\right|^2, \forall n \in \mathcal{N}, i, j \in \mathcal{N}, \pi(i) > \pi(j). \tag{5}$$

The inequalities in (5) can also ensure the successful SIC implemented at the stronger SU and achieve fairness among SUs.

To protect the QoS of the PU, the interference power constraint needs to be considered, given as

$$\sum_{n=1}^{N} \left|(\mathbf{h}_{k,I}^{H} + \mathbf{f}_{k,R}^{H}\mathbf{\Theta}\mathbf{g}_{SI})\mathbf{w}_n\right|^2 \leq p_{tol,k}, \forall k, \tag{6}$$

where the maximum interference that the kth PU can tolerate is denoted by $p_{tol,k}$.

The total system energy consumption consists of the transmit power and the circuit power consumption. The circuit power consumption denoted by P_c, which is from the circuit power consumed by the SBS, i.e., $P_c = P_{SBS}$, where P_{SBS} denote the power consumption of the SBS. In order to protect the transmitter, the maximum power constraint needs to be satisfied, which is given as

$$P_{tot} = \sum_{n=1}^{N} ||\mathbf{w}_n||^2 + P_c \leq P_{\max}. \tag{7}$$

B. Problem Formulation

In order to comprehensively investigate the tradeoff between EE and SE in the downlink IRS-assisted CRN with NOMA, a MOOP framework is adopted to simultaneously optimize those two objectives. EE is defined as the ratio of the system transmission rate to the total power consumption, while SE is defined as the ratio of the system throughput to the total transmission bandwidth. Accordingly, the EE and SE can be respectively expressed as

$$\eta_{EE} = \frac{\sum_{n=1}^{N} R_{n\to n}}{P_{tot}}, \tag{8a}$$

$$\eta_{SE} = \sum_{n=1}^{N} R_{n\to n}. \tag{8b}$$

The MOOP is formulated as

$$\mathbf{P}_0 : \max_{\mathbf{w},\mathbf{\Theta}} \ \eta_{SE}, \tag{9a}$$

$$\max_{\mathbf{w},\mathbf{\Theta}} \ \eta_{EE}, \tag{9b}$$

$$\text{s.t. } C1 : R_{j\to n} \geq R_{n\to n}, \pi(j) > \pi(n), j, n \in \mathcal{N} \tag{9c}$$

$$C2 : R_{n\to n} \geq R_{\min}, n \in \mathcal{N} \tag{9d}$$

$$C3 : |[\mathbf{\Theta}]_{mm}| \leq 1, \forall m, \tag{9e}$$

$$C4 : \pi \in \Omega, \tag{9f}$$

$$(5) - (7), \tag{9g}$$

where Ω in the constraint $C4$ represents the set of all $N!$ possible SIC decoding orders. The constraint $C1$ guarantees that the SIC can be employed successfully and the constraint $C2$ indicates the minimum quality

of service (QoS) requirement of each SU, where $R_{\min}$ is the minimum rate requirement. The constraint $C3$ is the reflection coefficients constraint. The constraint (5) is served as the SIC constraint which facilitates the successful SIC implementation at SUs. The constraint (6) guarantees that the maximum interference leakage at the kth PU is tolerable.

III. User Decoding Order Design

The design of an optimal decoding order is important in systems with NOMA that can guarantee the success of SIC. The users need to be sorted in an ascending or descending order based on the channel gains of each user. However, in IRS-assisted CRNs with NOMA, the order of the SU depends not only on the direct link but also on the reflection link, which is changed with the adjustment of IRS elements' phase shift. Thus, the optimal decoding order can be any one of the $N!$ possible decode orderings. However, the exhaustive search is highly complex for all $N!$ different decoding orders. Thus, a low complexity decoding order design is studied to obtain the SIC decoding order by maximizing the sum of the combined channel gains of each SU. The optimization problem of the decoding order is formulated as

$$\mathbf{P}_1: \max_{\mathbf{\Theta}} \sum_{n=1}^{N} \left|\mathbf{g}_{n,D}^H + \mathbf{g}_{n,R}^H \mathbf{\Theta} \mathbf{g}_{SI}\right|^2, \tag{10a}$$

$$\text{s.t. } |[\mathbf{\Theta}]_{mm}| \leq 1, \forall m. \tag{10b}$$

Let $\mathbf{v}_n = \begin{bmatrix} \text{diag}(\mathbf{g}_{n,R}^H)\mathbf{g}_{SI} \\ \mathbf{g}_{n,D}^H \end{bmatrix}$, $\mathbf{e} = [\beta_1 e^{j\theta_1}, \beta_2 e^{j\theta_2}, \ldots, \beta_M e^{j\theta_M}\ 1]^T$. Then, $\left|\mathbf{g}_{n,D}^H + \mathbf{g}_{n,R}^H \mathbf{\Theta} \mathbf{g}_{SI}\right|^2$ can be rewritten as $\text{Tr}\left(\mathbf{V}_n \mathbf{E}\right)$, where $\mathbf{V}_n = \mathbf{v}_n \mathbf{v}_n^H$, $\mathbf{E} = \mathbf{e}\mathbf{e}^H$, and $\text{Rank}(\mathbf{E}) = 1$. By exploiting the SDR to drop the rank-one constraint, the problem is relaxed as

$$\mathbf{P}_{1.1}: \max_{\mathbf{E}} \text{Tr}\left(\sum_{n=1}^{N} \mathbf{V}_n \mathbf{E}\right), \tag{11a}$$

$$\text{s.t. } \mathbf{E}\left(m, m\right) \geq 1, m \in \mathcal{M}, \tag{11b}$$

$$\mathbf{E}\left(M+1, M+1\right) = 1, \tag{11c}$$

$$\mathbf{E} \succeq 0. \tag{11d}$$

It is obvious that problem $\mathbf{P}_{1.1}$ is a standard semidefinite programming (SDP) problem, which can be solved by using the existing convex optimization toolbox [43]. Note that the optimal solution of problem $\mathbf{P}_1$ can be recovered via eigenvalue decomposition only if the optimal solution $\mathbf{E}^{\ddagger}$ is a rank-one positive semidefinite matrix. However, the solution obtained by SDR is generally not rank-one due to the relaxation

of the rank-one constraint. Thus, the Gaussian randomization method can be applied to construct a rank-one solution based on the higher-rank $\mathbf{E}^{\ddagger}$ [30]. Specifically, if Rank $\left(\mathbf{E}^{\ddagger}\right)$ is unequal to 1, the eigenvalue decomposition of $\mathbf{E}^{\ddagger}$ is defined as

$$\mathbf{E}^{\ddagger} = \mathbf{U}\mathbf{\Lambda}\mathbf{U}^{H}, \tag{12}$$

where $\mathbf{U}$ is the identity matrix of the eigenvectors, and $\mathbf{\Lambda}$ is the diagonal matrix of eigenvalues. Then, a suboptimal solution to $\mathbf{P}_{1.1}$ can be obtained as

$$\tilde{\mathbf{e}}_t = \mathbf{U}\mathbf{\Lambda}^{\frac{1}{2}}\boldsymbol{r}_t,\ t = 1, 2, \ldots, T, \tag{13}$$

where T denotes the maximum generation of candidate random variables and $\boldsymbol{r}_t \sim \mathcal{CN}\left(0, \mathbf{I}_{M+1}\right)$ is a random vector of the tth generation, which can be expressed as

$$\boldsymbol{r}_t = \boldsymbol{x} + \boldsymbol{y}i,\ t = 1, 2, \ldots, T, \tag{14}$$

where $\boldsymbol{x} \in \mathbb{R}^{(M+1)\times 1}$ and $\boldsymbol{y} \in \mathbb{R}^{(M+1)\times 1}$ are independent normally distributed random vectors with zero mean and covariance matrix $\frac{1}{2}\mathbf{I}_{M+1}$.

Thus, the candidate reflection matrix can be obtained as

$$\mathbf{\Theta}_t = \operatorname{diag}\left\{e^{j\angle\frac{\tilde{\mathbf{e}}_t[1]}{\tilde{\mathbf{e}}_t[M+1]}}, e^{j\angle\frac{\tilde{\mathbf{e}}_t[2]}{\tilde{\mathbf{e}}_t[M+1]}}, \ldots, e^{j\angle\frac{\tilde{\mathbf{e}}_t[M]}{\tilde{\mathbf{e}}_t[M+1]}}\right\}. \tag{15}$$

After obtaining the candidate set of reflection coefficient matrix $\{\mathbf{\Theta}_t\}$, the optimal reflection coefficient matrix can be found among them, which maximizes the combined channel gains of all SUs. The decoding order optimization algorithm is summarized in **Algorithm 1**.

IV. Multiple-Objective Optimization Design Under Perfect CSI

In this section, the downlink IRS-assisted CRNs with NOMA is studied under the perfect CSI. A MOO framework is introduced to investigate the trade-off between SE and EE with the given decoding order. Then, the ϵ-constraint method is adopted to transform the MOOP into a tractable SOOP. Finally, an effective BCD-based iterative algorithm is proposed to alternatively optimize the beamforming vectors and the phase shift matrix.

TABLE I

THE ALTERNATING OPTIMIZATION ALGORITHM

Algorithm 1: The alternating optimization algorithm

1: Solving the relaxed SDP problem $\mathbf{P}_{1.1}$;
2: **if** rank $\left(\mathbf{E}^{\ddagger}\right)=1$ **then**
3: Using the obtained $\mathbf{E}^{\ddagger}$ to calculate its eigenvalue λ_{eigen} and corresponding eigenvector $\boldsymbol{u}$ via eigen-decomposition;
4: Updating $\boldsymbol{\Theta}^{\ddagger}=\text{diag}\{\boldsymbol{u}\sqrt{\lambda_{eigen}}\}$;
5: **else**
6: Obtaining the eigenvalue decomposition according to (12);
7: **for** $t=1,2,\ldots,T$ **do**
8: Generating the Gaussian random vector r_t according to (14);
8: Calculating $\boldsymbol{\Theta}_t$ using (15);
9: Calculating the objective value of problem $\mathbf{P}_1$;
10: **end for**
11: **end if**
12: Let $\boldsymbol{\Theta}^{\ddagger}=\boldsymbol{\Theta}_{t^{\ddagger}}$, where $t^{\ddagger}$=arg $\max\limits_{t}\sum\limits_{n=1}^{N}\left|\mathbf{g}_{n,D}^{H}+\mathbf{g}_{n,R}^{H}\boldsymbol{\Theta}\mathbf{g}_{SI}\right|^{2}$;
13: Using the optimal $\boldsymbol{\Theta}^{\ddagger}$ to calculate all combined channel gains $\{\left|\mathbf{g}_{n,D}^{H}+\mathbf{g}_{n,R}^{H}\boldsymbol{\Theta}\mathbf{g}_{SI}\right|^{2},n\in\mathcal{N}\}$ and rank them in the ascending order;
14: **Output**: decoding order $\pi(n),n\in\mathcal{N}$.

A. Optimization Problem Formulation

For the decoding order obtained in Section III, the equality in the constraint $C1$ obviously always holds. Thus, the MOOP $\mathbf{P}_0$ can be rewritten as

$$\mathbf{P}_2:\max_{\mathbf{w},\boldsymbol{\Theta}}\ \eta_{SE}, \tag{16a}$$

$$\max_{\mathbf{w},\boldsymbol{\Theta}}\ \eta_{EE}, \tag{16b}$$

$$\text{s.t. } C2,C3,(6),(7), \tag{16c}$$

$$\left|\left(\mathbf{g}_{n,D}^{H}+\mathbf{g}_{n,R}^{H}\boldsymbol{\Theta}\mathbf{g}_{SI}\right)\mathbf{w}_i\right|^{2}\leq\left|\left(\mathbf{g}_{n,D}^{H}+\mathbf{g}_{n,R}^{H}\boldsymbol{\Theta}\mathbf{g}_{SI}\right)\mathbf{w}_j\right|^{2},\forall n\in\mathcal{N},i>j,i,j\in\mathcal{N}, \tag{16d}$$

where i, j and n denote the decoding index of the ith SU, the jth SU and the nth SU, respectively. Note that constraint (16d) can ensure the effectiveness of SIC. The achievable rate of the nth SU decoding its

own signal is given as

$$R_{n\to n}=\log_2\left(1+\frac{\left|\left(\mathbf{g}_{n,D}^H+\mathbf{g}_{n,R}^H\mathbf{\Theta}\mathbf{g}_{SI}\right)\mathbf{w}_n\right|^2}{\sum\limits_{i=n+1}^{N}\left|\left(\mathbf{g}_{n,D}^H+\mathbf{g}_{n,R}^H\mathbf{\Theta}\mathbf{g}_{SI}\right)\mathbf{w}_i\right|^2+\sum\limits_{k=1}^{K}\left|f_{n,D}^P+\mathbf{g}_{n,R}^H\mathbf{\Theta}\mathbf{f}_{PI}\right|^2p_k^P+n_j}\right). \tag{17}$$

It is evident that problem $\mathbf{P}_2$ is a challenging non-convex MOOP. Although the decoding order is determined, the objective function (16b) is a fractional function, and the beamforming vector and IRS phase shift matrix are highly coupled. In order to tackle the highly-coupled non-convex MOOP, we transform problem $\mathbf{P}_2$ into a SOOP and then decompose the original problem into two subproblems of beamforming optimization and reflection coefficients optimization. An alternative algorithm is proposed to tackle this challenging problem.

B. Problem Reformulation

To tackle the MOOP, the ϵ-constraint method is employed [40]. In particular, the EE maximization is kept as the objective function and the objective function of SE maximization is transformed into a constraint. Thus, the corresponding SOOP can be given as

$$\mathbf{P}_3:\max_{\mathbf{w},\mathbf{\Theta}}\ \eta_{EE}, \tag{18a}$$

$$\text{s.t. } \eta_{SE}\geq\epsilon, \tag{18b}$$

$$\text{(16c), (16d)}, \tag{18c}$$

where constraint (18b) guarantees the sum throughput of the secondary network is larger than ϵ.

Remark 1: The feasibility of $\mathbf{P}_4$ is significantly dependent on the value of ϵ. Note that the value of ϵ should be not larger than the maximum η_{SE} [41]. Thus, the ϵ can be specified as a value in $(0,\eta_{SE,\max}]$ after solely maximizing η_{SE}.

Due to the highly coupled variables and the fractional form of the objective function, the problem $\mathbf{P}_4$ is still non-convex and intractable. In order to solve this problem, a BCD-based iterative algorithm is proposed. The beamforming vectors are first optimized with the given phase shift matrix, then the phase shift matrix design is optimized with the obtained feasible beamforming vectors.

C. Beamforming Design for Given IRS Phase Shift

Let $\mathbf{W}_n = \mathbf{w}_n\mathbf{w}_n^H$, $\mathbf{W}_n \in \mathbb{H}^{N_s}$. For given $\mathbf{\Theta}$, the quadratic terms $\left|\left(\mathbf{g}_{n,D}^H + \mathbf{g}_{n,R}^H\mathbf{\Theta}\mathbf{g}_{SI}\right)\mathbf{w}_n\right|^2$ and $\left|f_{n,D}^P + \mathbf{g}_{n,R}^H\mathbf{\Theta}\mathbf{f}_{PI}\right|^2$ in (17), and the term $\left|(\mathbf{h}_{k,I}^H + \mathbf{f}_{k,R}^H\mathbf{\Theta}\mathbf{g}_{SI})\mathbf{w}_n\right|^2$ in (6) are rewritten as, respectively,

$$\left|\left(\mathbf{g}_{n,D}^H + \mathbf{g}_{n,R}^H\mathbf{\Theta}\mathbf{g}_{SI}\right)\mathbf{w}_n\right|^2 = \left|\mathbf{e}^H\mathbf{v}_n\mathbf{w}_n\right|^2 = \mathrm{Tr}(\mathbf{W}_n\mathbf{v}_n^H\mathbf{e}\mathbf{e}^H\mathbf{v}_n), \tag{19a}$$

$$\left|f_{n,D}^P + \mathbf{g}_{n,R}^H\mathbf{\Theta}\mathbf{f}_{PI}\right|^2 = \left|f_{n,D}^P + \mathbf{e}^H\mathbf{f}_n\right|^2 = \left|\vartheta_n\right|^2, \tag{19b}$$

$$\left|(\mathbf{h}_{k,I}^H + \mathbf{f}_{k,R}^H\mathbf{\Theta}\mathbf{g}_{SI})\mathbf{w}_n\right|^2 = \left|\mathbf{e}^H\mathbf{H}_k\mathbf{w}_n\right|^2 = \mathrm{Tr}\left(\mathbf{W}_n\mathbf{H}_k^H\mathbf{e}\mathbf{e}^H\mathbf{H}_k\right), \tag{19c}$$

where $\mathbf{e} = [\beta_1 e^{j\theta_1}, \beta_2 e^{j\theta_2}, \ldots, \beta_M e^{j\theta_M}\ 1]^T$, $\mathbf{v}_n = \begin{bmatrix} \mathrm{diag}(\mathbf{g}_{n,R}^H)\mathbf{g}_{SI} \\ \mathbf{g}_{n,D}^H \end{bmatrix}$, $\mathbf{f}_n = \mathrm{diag}(\mathbf{g}_{n,R}^H)\mathbf{f}_{SI}$, $\vartheta_n = f_{n,D}^P + \mathbf{e}^H\mathbf{f}_n$ and $\mathbf{H}_k = \begin{bmatrix} \mathrm{diag}(\mathbf{f}_{k,R}^H)\mathbf{g}_{SI} \\ \mathbf{h}_{k,I}^H \end{bmatrix}$, respectively. Then, the achievable SINR at the nth SU to decode its own signal can be rewritten as

$$\mathrm{SINR}_{n\to n} = \frac{\mathrm{Tr}(\mathbf{W}_n\mathbf{v}_n^H\mathbf{e}\mathbf{e}^H\mathbf{v}_n)}{\sum\limits_{i=n+1}^{N}\mathrm{Tr}(\mathbf{W}_i\mathbf{v}_n^H\mathbf{e}\mathbf{e}^H\mathbf{v}_n) + |\vartheta_n|^2 p_k^P + \sigma^2}. \tag{20}$$

Then, the active beamforming optimization can be formulated as

$$\mathbf{P}_{3.1}: \max_{\mathbf{W}_n} \frac{\sum\limits_{n=1}^{N} R_{n\to n}}{\sum\limits_{n=1}^{N}\mathrm{Tr}\left(\mathbf{W}_n\right) + p_c}, \tag{21a}$$

$$\text{s.t. } C2, (18b), \tag{21b}$$

$$\sum_{n=1}^{N}\mathrm{Tr}\left(\mathbf{W}_n\right) + p_c \le P_{\max}, \tag{21c}$$

$$\sum_{n=1}^{N}\mathrm{Tr}\left(\mathbf{W}_n\mathbf{H}_k^H\mathbf{e}\mathbf{e}^H\mathbf{H}_k\right) \le p_{tol,k}, \forall k, \tag{21d}$$

$$\mathrm{Tr}(\mathbf{W}_i\mathbf{v}_n^H\mathbf{e}\mathbf{e}^H\mathbf{v}_n) \le \mathrm{Tr}(\mathbf{W}_j\mathbf{v}_n^H\mathbf{e}\mathbf{e}^H\mathbf{v}_n), i > j, \forall n, i, j \in \mathcal{N}, \tag{21e}$$

$$\mathbf{W}_n \succeq 0, \forall n, \tag{21f}$$

$$\mathrm{Rank}\left(\mathbf{W}_n\right) = 1, \forall n. \tag{21g}$$

Note that constraints (21g) and (21h) are imposed to guarantee that $\mathbf{W}_n = \mathbf{w}_n\mathbf{w}_n^H$ holds after optimization. Problem $\mathbf{P}_{3.1}$ is a non-convex problem due to the fractional form of the objective function and the non-convexity of the constraints (21b) and (21d). To tackle the problem $\mathbf{P}_{3.1}$, we introduce auxiliary variables

α and $\boldsymbol{\gamma} = \{\gamma_1, \ldots, \gamma_N\}$. The equivalent problem can be given as

$$\mathbf{P}_{3.2}: \max_{\mathbf{W}_n, \alpha, \boldsymbol{\gamma}} \quad \alpha, \tag{22a}$$

$$\text{s.t. (21b)} - \text{(21g)}, \tag{22b}$$

$$\frac{\sum_{n=1}^{N} \log_2(1+\gamma_n)}{\sum_{n=1}^{N} \text{Tr}(\mathbf{W}_n) + p_c} \geq \alpha, \tag{22c}$$

$$\text{SINR}_{n\to n} \geq \gamma_n, \forall n. \tag{22d}$$

Although the objective function (22a) is linear, the problem $\mathbf{P}_{3.2}$ is still non-convex. The non-convexity originates from the constrains (22c), (22d) and the rank-one constraint (21g). To deal with the non-convex constraint (22c), we first rewrite it as $\sum_{n=1}^{N} \log_2(1+\gamma_n) \geq \alpha \sum_{n=1}^{N} \text{Tr}(\mathbf{W}_n) + \alpha p_c$. The first right hand term $\alpha \sum_{n=1}^{N} \text{Tr}(\mathbf{W}_n)$ is the joint convex function with respect to α and $\mathbf{W}_n$. By performing the first-order Taylor approximation, the lower bound of $f(\alpha, \mathbf{W}_n) \triangleq \alpha \sum_{n=1}^{N} \text{Tr}(\mathbf{W}_n)$ for a given feasible point $(\alpha^l, \mathbf{W}_n^l)$ in the lth iteration of the SCA is expressed as

$$\begin{aligned} f(\alpha, \mathbf{W}_n) &\geq f(\alpha^l, \mathbf{W}_n^l) + \sum_{n\in\mathcal{N}} \text{Tr}\left(\bigtriangledown_{\mathbf{W}_n} f(\alpha^l, \mathbf{W}_n^l)^H (\mathbf{W}_n - \mathbf{W}_n^l)\right) + \bigtriangledown_{\alpha} f(\alpha^l, \mathbf{W}_n^l)(\alpha - \alpha^l) \\ &\triangleq \widehat{f}(\alpha, \mathbf{W}_n). \end{aligned} \tag{23}$$

Then, concerning the constraint (22d), we further introduce a set of auxiliary variables $I_n, \forall n \in \mathcal{N}$ as the interference-plus-noise power of the data transmission of the nth SU. Hence, constraint (22d) can be transformed as

$$\text{Tr}(\mathbf{W}_n \mathbf{v}_n^H \mathbf{e}\mathbf{e}^H \mathbf{v}_n) \geq \gamma_n I_n, \tag{24a}$$

$$\sum_{i=n+1}^{N} \text{Tr}(\mathbf{W}_i \mathbf{v}_n^H \mathbf{e}\mathbf{e}^H \mathbf{v}_n) + |\vartheta_n|^2 p_k^P + \sigma^2 \leq I_n. \tag{24b}$$

Similarly, in the lth iteration of the SCA, a lower bound of $\gamma_n I_n$ in constraint (24a) at a given point (γ_n^l, I_n^l) can be constructed as

$$\gamma_n I_n \geq \gamma_n^l {I_n}^l + \gamma_n^l (I_n - {I_n}^l) + {I_n}^l (\gamma_n - \gamma_n^l) \triangleq \widehat{f}(\gamma_n I_n). \tag{25}$$

Then, the original problem $\mathbf{P}_{3.1}$ is approximated as

$$\mathbf{P}_{3.3}: \max_{\mathbf{W}_n,\alpha,\boldsymbol{\gamma},\boldsymbol{I}} \ \alpha, \tag{26a}$$

$$\text{s.t. (21b)} - \text{(21g)}, \tag{26b}$$

$$\sum_{n=1}^{N} \log_2\left(1+\gamma_n\right) \geq \widehat{f}(\alpha, \mathbf{W}_n) + \alpha p_c, \tag{26c}$$

$$\text{Tr}(\mathbf{W}_n \mathbf{v}_n^H \mathbf{e}\mathbf{e}^H \mathbf{v}_n) \geq \widehat{f}(\gamma_n I_n), \forall n, \tag{26d}$$

$$\sum_{i=n+1}^{N} \text{Tr}(\mathbf{W}_i \mathbf{v}_n^H \mathbf{e}\mathbf{e}^H \mathbf{v}_n) + |\vartheta_n|^2 p_k^P + \sigma^2 \leq I_n, \forall n. \tag{26e}$$

Note that the remaining non-convexity of problem $\mathbf{P}_{3.3}$ is caused by the rank-one constraint (21g). Hence, the SDR method is adopted to relax the rank-one constraint [42]. Finally, the relaxed problem of problem $\mathbf{P}_{3.3}$ is a convex semidefinite program (SDP), which can be optimally solved via standard convex solvers such as CVX [43]. To verify the tightness of SDR, **Theorem 1** is given.

***Theorem** 1:* The optimal solution of problem $\mathbf{P}_{3.3}$ without the rank-one constraint can always satisfy $\text{rank}(\mathbf{W}_n) \leq 1, \forall n \in \mathcal{N}$.

Proof: Please refer to Appendix A. ■

Note that the obtained objective function of problem $\mathbf{P}_{3.3}$ is served as a lower bound of that in the problem $\mathbf{P}_{3.1}$ owing to the replacement of the constraints (26b) and (26c). Let $\mathbf{W}_n^{\ddagger}, \forall n$ denote the optimal solution of problem $\mathbf{P}_{3.3}$. Since $\mathbf{W}_n^{\ddagger} = \mathbf{w}_n^{\ddagger}\mathbf{w}_n^{\ddagger H}$, the optimal beamforming vector $\mathbf{w}_n^{\ddagger}$ can be obtained by utilizing eigenvalue decomposition.

D. Phase Shift Optimization with Given Beamforming Vector

For given $\mathbf{w}_n$, the IRS phase shift optimization problem can be written as

$$\mathbf{P}_{3.4}: \max_{\boldsymbol{\Theta}} \ \eta_{SE}, \tag{27a}$$

$$\text{s.t. } C2, C3, (6), (16\text{d}), (18\text{b}). \tag{27b}$$

Note that the objective function and constraints are non-convex with respect to $\boldsymbol{\Theta}$. Therefore, the following transformation is performed to make the optimization problem more tractable.

Recall $\mathbf{W}_n = \mathbf{w}_n\mathbf{w}_n^H$, $\mathbf{e} = [\beta_1 e^{j\theta_1}, \beta_2 e^{j\theta_2}, \ldots, \beta_M e^{j\theta_M}\ 1]^T$, $\mathbf{v}_n = \begin{bmatrix} \text{diag}(\mathbf{g}_{n,R}^H)\mathbf{g}_{SI} \\ \mathbf{g}_{n,D}^H \end{bmatrix}$, $\mathbf{f}_n = \text{diag}(\mathbf{g}_{n,R}^H)\mathbf{f}_{SI}$, and $\mathbf{H}_k = \begin{bmatrix} \text{diag}(\mathbf{f}_{k,R}^H)\mathbf{g}_{SI} \\ \mathbf{h}_{k,I}^H \end{bmatrix}$. To tackle the non-convexity in $\mathbf{P}_{3.4}$, the quadratic term $\left|\left(\mathbf{g}_{n,D}^H + \mathbf{g}_{n,R}^H \boldsymbol{\Theta} \mathbf{g}_{SI}\right)\mathbf{w}_n\right|^2$ in (17) is rewritten as

$$\left|\left(\mathbf{g}_{n,D}^H + \mathbf{g}_{n,R}^H \boldsymbol{\Theta} \mathbf{g}_{SI}\right)\mathbf{w}_n\right|^2 = \text{Tr}\left(\mathbf{e}^H \mathbf{v}_n \mathbf{W}_n \mathbf{v}_n^H \mathbf{e}\right) = \text{Tr}\left(\mathbf{E}\mathbf{v}_n \mathbf{W}_n \mathbf{v}_n^H\right), \tag{28}$$

where $\mathbf{E} \triangleq \mathbf{e}\mathbf{e}^H, \mathbf{E} \in \mathbb{C}^{(M+1)\times(M+1)}$. Similarly, the term $\left|f_{n,D}^P + \mathbf{g}_{n,R}^H \mathbf{\Theta} \mathbf{f}_{PI}\right|^2$ in (17) and the term $\left|(\mathbf{h}_{k,I}^H + \mathbf{f}_{k,R}^H \mathbf{\Theta} \mathbf{g}_{SI})\mathbf{w}_n\right|^2$ in (6) are rewritten as, respectively

$$\left|f_{n,D}^P + \mathbf{g}_{n,R}^H \mathbf{\Theta} \mathbf{f}_{PI}\right|^2 = \text{Tr}\left(\mathbf{E}\mathbf{F}_n\right), \tag{29a}$$

$$\left|(\mathbf{h}_{k,I}^H + \mathbf{f}_{k,R}^H \mathbf{\Theta} \mathbf{g}_{SI})\mathbf{w}_n\right|^2 = \text{Tr}\left(\mathbf{E}\mathbf{H}_k \mathbf{W}_n \mathbf{H}_k^H\right), \tag{29b}$$

where $\mathbf{F}_n$ is defined as

$$\mathbf{F}_n = \begin{bmatrix} \mathbf{f}_n \mathbf{f}_n^H & f_{n,D}^{*P} \mathbf{f}_n \\ \mathbf{f}_n^H f_{n,D}^P & \left|f_{n,D}^P\right|^2 \end{bmatrix}. \tag{30}$$

Then, the IRS phase shift optimization problem can be rewritten as

$$\mathbf{P}_{3.5}: \max_{\mathbf{E}} \frac{1}{P_{tot}} \sum_{n=1}^{N} \log_2 \left(1 + \frac{\text{Tr}\left(\mathbf{E}\mathbf{v}_n \mathbf{W}_n \mathbf{v}_n^H\right)}{\sum\limits_{i=n+1}^{N} \text{Tr}\left(\mathbf{E}\mathbf{v}_n \mathbf{W}_i \mathbf{v}_n^H\right) + \sum\limits_{k=1}^{K} \text{Tr}\left(\mathbf{E}\mathbf{F}_n\right) p_k^P + n_j}\right), \tag{31a}$$

$$\text{s.t. } C2, (18b), \tag{31b}$$

$$\sum_{n=1}^{N} \text{Tr}\left(\mathbf{E}\mathbf{H}_k \mathbf{W}_n \mathbf{H}_k^H\right) \leq p_{tol,k}, \forall k, \tag{31c}$$

$$\text{Tr}\left(\mathbf{E}\mathbf{v}_n \mathbf{W}_i \mathbf{v}_n^H\right) \leq \text{Tr}\left(\mathbf{E}\mathbf{v}_n \mathbf{W}_j \mathbf{v}_n^H\right), i > j, \forall n, i, j \in \mathcal{N}, \tag{31d}$$

$$\mathbf{E} \succeq 0, \tag{31e}$$

$$\text{Rank}\left(\mathbf{E}\right) = 1, \forall n, \tag{31f}$$

where constraints (31e) and (31f) ensure that $\mathbf{E} = \mathbf{e}\mathbf{e}^H$ holds after optimization. The problem $\mathbf{P}_{3.5}$ is non-convex owing to the non-convex objective function and constraint (31b) and (31f). Similar to the method adopted for solving problem $\mathbf{P}_{3.1}$, by applying SDR and introducing auxiliary variables Γ_n and z_n, the problem $\mathbf{P}_{3.5}$ can be transformed into

$$\mathbf{P}_{3.6}: \max_{\mathbf{E},\mathbf{\Gamma},\boldsymbol{z}} \frac{1}{P_{tot}} \sum_{n=1}^{N} \log_2 \left(1 + \Gamma_n\right), \tag{32a}$$

$$\text{s.t. } (31b) - (31e), \tag{32b}$$

$$\text{Tr}\left(\mathbf{E}\mathbf{v}_n \mathbf{W}_n \mathbf{v}_n^H\right) \geq \Gamma_n z_n, \forall n, \tag{32c}$$

$$\sum_{i=n+1}^{N} \text{Tr}\left(\mathbf{E}\mathbf{v}_n \mathbf{W}_i \mathbf{v}_n^H\right) + \sum_{k=1}^{K} \text{Tr}\left(\mathbf{E}\mathbf{F}_n\right) p_k^P + n_j \leq z_n, \forall n. \tag{32d}$$

Since variables in the right hand term of constraint (32c) is coupled, the SCA is applied to tackle the non-convexity of constraint (32c). Thus, in the lth iteration of the SCA, the lower bound with the first-order

Taylor approximation at the given feasible point (Γ_n^l, z_n^l) can be given as

$$\Gamma_n z_n \geq \Gamma_n^l {z_n}^l + \Gamma_n^l (z_n - {z_n}^l) + {z_n}^l (\Gamma - \Gamma_n^l) \triangleq \widehat{f}(\Gamma_n z_n). \tag{33}$$

Then, a lower bound of the problem $\mathbf{P}_{3.6}$ can be obtained by solving the following problem, given as

$$\mathbf{P}_{3.7}: \max_{\mathbf{E},\mathbf{\Gamma},\boldsymbol{z}} \frac{1}{P_{tot}} \sum_{n=1}^{N} \log_2 (1 + \Gamma_n), \tag{34a}$$

$$\text{s.t. } (31\text{b}) - (31\text{e}), (32\text{d}), \tag{34b}$$

$$\text{Tr}\left(\mathbf{E}\mathbf{v}_n \mathbf{W}_n \mathbf{v}_n^H\right) \geq \widehat{f}(\Gamma_n z_n), \forall n. \tag{34c}$$

The problem $\mathbf{P}_{3.7}$ is a standard SDP problem and the optimal $\mathbf{E}^{\ddagger}$ can be obtained by using the standard convex optimization toolboxes such as CVX [43]. Finally, since $\mathbf{E}^{\ddagger} = \mathbf{e}^{\ddagger}\mathbf{e}^{\ddagger H}$, $\mathbf{e}^{\ddagger}$ can be obtained by eigenvalue decomposition if the rank of $\mathbf{E}^{\ddagger}$ is one. Otherwise, the Gaussian randomization can be adopted to alternatively obtain the approximate $\mathbf{e}$ [42]. Therefore, the BCD-based iterative algorithm for solving the problem $\mathbf{P}_3$ can be summarized in **Algorithm 2**.

V. Multiple-Objective Optimization Design Under Imperfect CSI

In this section, the SE-EE tradeoff design is extended into a more practical IRS-assisted MISO CRN with NOMA, where the CSI between the SBS and primary network are imperfect. The SE-EE tradeoff is investigated by jointly optimizing beamforming vector and the phase shift matrix. Under the bounded error model, a robust resource allocation strategy is proposed.

A. Imperfect Channel Model

In practice, due to the limit cooperation between the secondary network and the primary network, the channel information of the SBS-PUs link and the IRS-PUs link cannot be accurately obtained. Specifically, the PUs may not directly interact with the SBS in practice. The imperfect CSI can also be caused by channel estimation and quantization errors. Thus, the worst-case channel uncertainty model is considered to capture the impact of the imperfect CSI. The bounded CSI error models for the channel vector $\mathbf{h}_{k,I}$ and $\mathbf{f}_{k,R}$ are given as

$$\mathbf{h}_{k,I} = \bar{\mathbf{h}}_{k,I} + \Delta\mathbf{h}_{k,I}, \tag{35a}$$

$$\mathcal{H}_{k,I} \triangleq \left\{\Delta\mathbf{h}_{k,I} \in \mathbb{C}^{N_s \times 1} : \Delta\mathbf{h}_{k,I}^H \Delta\mathbf{h}_{k,I} \leq \xi_{k,I}^2\right\}, \tag{35b}$$

$$\mathbf{f}_{k,R} = \bar{\mathbf{f}}_{k,R} + \Delta\mathbf{f}_{k,R}, \tag{35c}$$

$$\mathcal{F}_{k,R} \triangleq \left\{\Delta\mathbf{f}_{k,R} \in \mathbb{C}^{M \times 1} : \Delta\mathbf{f}_{k,R}^H \Delta\mathbf{f}_{k,R} \leq \xi_{k,R}^2\right\}, \tag{35d}$$

TABLE II

THE BCD-BASED ITERATIVE ALGORITHM

Algorithm 2: The BCD-based iterative algorithm

1: Set initial points $\mathbf{W}_n^1$ and $\mathbf{E}^1$, iteration index $q = 1$, and convergence tolerance $0 \leq \varepsilon_{BCD} \ll 1$;
2: **repeat**
3: Set iteration index $l = 1$ and error tolerance $0 \leq \varepsilon_{SCA} \ll 1$;
4: **repeat**
5: Solving the problem $\mathbf{P}_{3.2}$ for given $\mathbf{E}^q, \mathbf{W}_n^l$, α^l, γ^l and I_n^l;
6: Storing the intermediate solution $\mathbf{W}_n$;
7: Updating $l = l + 1$, $\mathbf{W}_n^{l+1} = \mathbf{W}_n$, $\alpha^{l+1}, \gamma^{l+1}$ and I_n^{l+1};
8: **until** $\frac{|\alpha^l - \alpha^{l-1}|}{|\alpha^l|} \leq \varepsilon_{SCA}$
9: Obtaining $\mathbf{W}_n^q = \mathbf{W}_n^l$;
10: **repeat**
11: Set iteration index $l = 1$;
12: Obtained the $\mathbf{E}$ by solving the problem $\mathbf{P}_{3.7}$ for the given $\mathbf{W}_n^q, \Gamma_n^l$ and $\mathbf{z}_n^l$;
13: Updating $l = l + 1$, $\mathbf{E}^{l+1} = \mathbf{E}$, Γ_n^{l+1} and $\mathbf{z}_n^{l+1}$;
14: **until** $\frac{\left|\frac{1}{P_{tot}} \sum\limits_{n \in N} \log_2\left(1+\Gamma_n^l\right) - \frac{1}{P_{tot}} \sum\limits_{n \in N} \log_2\left(1+\Gamma_n^{l-1}\right)\right|}{\left|\frac{1}{P_{tot}} \sum\limits_{n=1}^{N} \log_2\left(1+\Gamma_n^l\right)\right|} \leq \varepsilon_{SCA}$;
15: Obtaining $\mathbf{E}^q = \mathbf{E}^l$ and recovering $\mathbf{\Theta}^q$;
16: Set $q = q + 1$;
17: **until** $\left|\frac{\eta_{EE}^q}{\eta_{EE}^{q-1} - 1}\right| \leq \varepsilon_{BCD}$;
18: Obtaining $\mathbf{W}_n^\ddagger = \mathbf{W}_n^q$ and $\mathbf{\Theta}^\ddagger = \mathbf{\Theta}^q$.

where $\bar{\mathbf{h}}_{k,I}$ and $\bar{\mathbf{f}}_{k,R}$ are the estimates of $\mathbf{h}_{k,I}$ and $\mathbf{f}_{k,R}$, respectively. The uncertainty regions of the channel vectors $\mathbf{h}_{k,I}$ and $\mathbf{f}_{k,R}$ are denoted by $\mathcal{H}_{k,I}$ and $\mathcal{F}_{k,R}$, respectively. $\Delta\mathbf{h}_{k,I}$ and $\Delta\mathbf{h}_{k,I}$ represent the channel estimation errors of $\mathbf{h}_{k,I}$ and $\mathbf{f}_{k,R}$. $\xi_{k,I}$ and $\xi_{k,R}$ are the radius of the uncertainty regions $\mathcal{H}_{k,I}$ and $\mathcal{F}_{k,R}$, respectively, which are known by the SBS.

By considering the imperfect CSI, we aim to simultaneously maximize the worst-case SE and EE of the secondary network in IRS-assisted CRNs with NOMA by jointly optimizing beamforming vectors and IRS phase shifts. With the given decoding order, the corresponding optimization problem is formulated

as

$$\mathbf{P}_4: \max_{\mathbf{w},\mathbf{\Theta}} \ \eta_{SE}, \tag{36a}$$

$$\max_{\mathbf{w},\mathbf{\Theta}} \ \eta_{EE}, \tag{36b}$$

$$\text{s.t. } C2, C3, (6), (7), (16\text{d}), \tag{36c}$$

$$\max_{\substack{\mathbf{h}_{k,I}^H \in \mathcal{H}_{k,I} \\ \mathbf{f}_{k,R} \in \mathcal{F}_{k,R}}} \sum_{n \in N} \left| \mathbf{h}_{k,I}^H \mathbf{w}_n + \mathbf{f}_{k,R}^H \mathbf{\Theta} \mathbf{g}_{SI} \mathbf{w}_n \right|^2 \leq p_{tol,k}, \forall k. \tag{36d}$$

Note that the main challenge for solving the problem $\mathbf{P}_4$ is the semi-infinite constraint (36d) imposed by the uncertain regions $\mathcal{H}_{k,I}$ and $\mathcal{F}_{k,R}$. Besides, the coupling variables and non-convexity of both the objective functions and constraints are challenging to efficiently obtain the optimal solution. Thus, an approximation is firstly employed to transform constraint (36d) into the convex constraints. Then, using the method for solving $\mathbf{P}_3$, the challenging non-convex problem $\mathbf{P}_4$ can be also solved by the BCD-based iterative algorithm.

B. Transformation of the Semi-Infinite Constraint

In order to tackle the CSI uncertainties, it is generally expected to transform the semi-infinite constraints into equivalent linear matrix inequalities (LMIs) [39]. However, constraint (36d) contains the coupling variables and the cascaded channel of direct and reflecting links. Thus, a safe approximation is adopted to transform the constraint (36d) into a set of constraints that are convex over $\mathbf{w}_n$ and $\mathbf{\Theta}$ [36]. First, by applying the inequality $|a+b+c|^2 \leq 3|a|^2 + 3|b|^2 + 3|c|^2$ for obtaining an upper bound of constraint (36d), one has

$$(36\text{d}) \Rightarrow \max_{\substack{\mathbf{h}_{k,I}^H \in \mathcal{H}_{k,I} \\ \mathbf{f}_{k,R} \in \mathcal{F}_{k,R}}} \sum_{n \in N} \left(\left| \bar{\mathbf{h}}_{k,I}^H \mathbf{w}_n + \bar{\mathbf{f}}_{k,R}^H \mathbf{\Theta} \mathbf{g}_{SI} \mathbf{w}_n \right|^2 + \left| \Delta \mathbf{h}_{k,I}^H \mathbf{w}_n \right|^2 + \left| \Delta \mathbf{f}_{k,R}^H \mathbf{\Theta} \mathbf{g}_{SI} \mathbf{w}_n \right|^2 \right) \leq \frac{p_{tol,k}}{3}, \forall k, \tag{37}$$

Then, by introducing slack variables ς and κ, the inequations (37) can be further equivalent to the following constraints

$$\max_{\mathbf{h}_{k,I}^H \in \mathcal{H}_{k,I}} \sum_{n \in N} \left| \Delta \mathbf{h}_{k,I}^H \mathbf{w}_n \right|^2 + \varsigma_k \leq \frac{p_{tol,k}}{3}, \tag{38a}$$

$$\max_{\mathbf{f}_{k,R} \in \mathcal{F}_{k,R}} \sum_{n \in N} \left| \Delta \mathbf{f}_{k,R}^H \mathbf{\Theta} \mathbf{g}_{SI} \mathbf{w}_n \right|^2 + \kappa_k \leq \varsigma_k, \tag{38b}$$

$$\sum_{n \in N} \left| \bar{\mathbf{h}}_{k,I}^H \mathbf{w}_n + \bar{\mathbf{f}}_{k,R}^H \mathbf{\Theta} \mathbf{g}_{SI} \mathbf{w}_n \right|^2 \leq \kappa_k. \tag{38c}$$

It can be observed that (38c) is convex with respect to $\mathbf{w}_n$ and $\mathbf{\Theta}$, while (38a) and (38b) are semi-infinite constraints. Thus, the $\mathcal{S}$-Procedure is applied to make the problem tractable, which is expressed as follows.

Lemma 1: (*$\mathcal{S}$-Procedure*) [44]: Let a function $f_m(\mathbf{z}) = \mathbf{z}^H \mathbf{A}_m \mathbf{z} + 2\Re\{\mathbf{b}_m^H \mathbf{z}\} + c_m$, $m \in \{1, 2\}$, where $\mathbf{z} \in \mathbb{C}^{N\times 1}$, $\mathbf{A}_m \in \mathbb{H}^N$, $\mathbf{b}_m \in \mathbb{C}^{N\times 1}$, and $c_m \in \mathbb{R}$. Then, the implication $f_1(\mathbf{z}) \geq 0 \Rightarrow f_2(\mathbf{z}) \geq 0$ holds if and only if there exists a $\delta \geq 0$ such that

$$\delta \begin{bmatrix} \mathbf{A}_1 & \mathbf{b}_1 \\ \mathbf{b}_1^H & c_1 \end{bmatrix} - \begin{bmatrix} \mathbf{A}_2 & \mathbf{b}_2 \\ \mathbf{b}_2^H & c_2 \end{bmatrix} \succeq \mathbf{0}, \tag{39}$$

provided that there exists a vector $\widehat{\mathbf{z}}$ such that $f_m(\widehat{\mathbf{z}}) < 0$.

Let $\mathbf{W}_n = \mathbf{w}_n \mathbf{w}_n^H$. By applying Lemma 1, constraint (38a) can be rewritten as

$$\begin{bmatrix} \delta_k \mathbf{I}_{N_s} - \sum\limits_n \mathbf{W}_n & \mathbf{0} \\ \mathbf{0} & -\delta_k \xi_{k,I}^2 - \varsigma_k + \frac{p_{tol,k}}{3} \end{bmatrix} \succeq \mathbf{0}. \tag{40}$$

Similarly, constraint (38b) can be rewritten as

$$\begin{bmatrix} \iota_k \mathbf{I}_M - \mathbf{\Theta} \sum\limits_{n\in N} \mathbf{g}_{SI} \mathbf{W}_n \mathbf{g}_{SI}^H \mathbf{\Theta}^H & \mathbf{0} \\ \mathbf{0} & -\iota_k \xi_{k,R}^2 - \kappa_k + \varsigma_k \end{bmatrix} \succeq \mathbf{0}, \forall k. \tag{41}$$

Note that both (40) and (41) are convex with respect to $\mathbf{W}_n$, while (41) is still non-convex with respect to $\mathbf{\Theta}$ due to the quadratic term $\mathbf{\Theta} \sum\limits_{n\in N} \mathbf{g}_{SI} \mathbf{W}_n \mathbf{g}_{SI}^H \mathbf{\Theta}^H$.

Moreover, let $\bar{\mathbf{H}}_k = \begin{bmatrix} \text{diag}(\bar{\mathbf{f}}_{k,R}^H)\mathbf{g}_{SI} \\ \bar{\mathbf{h}}_{k,I}^H \end{bmatrix}$ and $\mathbf{e} = [\beta_1 e^{j\theta_1}, \beta_2 e^{j\theta_2}, \ldots, \beta_M e^{j\theta_M}\ 1]^T$, constraint (39c) can be expressed as

$$\sum_{n\in N} \text{Tr}(\mathbf{W}_n \bar{\mathbf{H}}_k^H \mathbf{e}\mathbf{e}^H \bar{\mathbf{H}}_k) \leq \kappa_k. \tag{42}$$

C. Beamforming Design for Given IRS Phase Shift

Recall $\mathbf{W}_n = \mathbf{w}_n \mathbf{w}_n^H$, $\mathbf{e} = [\beta_1 e^{j\theta_1}, \beta_2 e^{j\theta_2}, \ldots, \beta_M e^{j\theta_M}\ 1]^T$, $\mathbf{v}_n = \begin{bmatrix} \text{diag}(\mathbf{g}_{n,R}^H)\mathbf{g}_{SI} \\ \mathbf{g}_{n,D}^H \end{bmatrix}$, $\mathbf{f}_n = \text{diag}(\mathbf{g}_{n,R}^H)\mathbf{f}_{SI}$, $\vartheta_n = f_{n,D}^P + \mathbf{e}^H \mathbf{f}_n$ and $\mathbf{H}_k = \begin{bmatrix} \text{diag}(\mathbf{f}_{k,R}^H)\mathbf{g}_{SI} \\ \mathbf{h}_{k,I}^H \end{bmatrix}$. Based on the transformation of constraint (36d), the

beamforming vector optimization with the given phase shifts can be expressed as

$$\mathbf{P}_{4.1}: \max_{\mathbf{W}_n,\varsigma,\kappa} \frac{\sum_{n=1}^{N} R_{n\to n}}{\sum_{n=1}^{N} \mathrm{Tr}\left(\mathbf{W}_n\right) + p_c}, \tag{43a}$$

$$\text{s.t. } C2, (18\text{b}), (40)-(42), \tag{43b}$$

$$\sum_{n=1}^{N} \mathrm{Tr}\left(\mathbf{W}_n\right) + p_c \le P_{\max}, \tag{43c}$$

$$\mathrm{Tr}(\mathbf{W}_i \mathbf{v}_n^H \mathbf{e}\mathbf{e}^H \mathbf{v}_n) \le \mathrm{Tr}(\mathbf{W}_j \mathbf{v}_n^H \mathbf{e}\mathbf{e}^H \mathbf{v}_n), i > j, \forall n, i, j \in \mathcal{N}, \tag{43d}$$

$$\mathbf{W}_n \succeq 0, \forall n, \tag{43e}$$

$$\mathrm{Rank}\left(\mathbf{W}_n\right) = 1, \forall n. \tag{43f}$$

The problem $\mathbf{P}_{4.1}$ is a non-convex problem due to both objective function and constraints. Similar to the previous section, by introducing the auxiliary variables ζ, $\boldsymbol{\chi}$, and $\boldsymbol{\rho}$ and utilizing SCA, the problem $\mathbf{P}_{4.1}$ can be approximated as

$$\mathbf{P}_{4.2}: \max_{\mathbf{W}_n,\zeta,\boldsymbol{\chi},\boldsymbol{\rho},\varsigma,\kappa} \quad \zeta, \tag{44a}$$

$$\text{s.t. } \sum_{n=1}^{N} \log_2\left(1+\chi_n\right) \ge \widehat{f}(\zeta, \mathbf{W}_n) + \zeta p_c, \tag{44b}$$

$$\mathrm{Tr}(\mathbf{W}_n \mathbf{v}_n^H \mathbf{e}\mathbf{e}^H \mathbf{v}_n) \ge \widehat{f}(\chi_n \rho_n), \forall n, \tag{44c}$$

$$\sum_{i=n+1}^{N} \mathrm{Tr}(\mathbf{W}_i \mathbf{v}_n^H \mathbf{e}\mathbf{e}^H \mathbf{v}_n) + |\vartheta_n|^2 p_k^P + \sigma^2 \le I_n, \forall n \tag{44d}$$

$$(43\text{b})-(43\text{f}), \tag{44e}$$

where $\widehat{f}(\zeta, \mathbf{W}_n)$ and $\widehat{f}(\chi_n \rho_n)$ are respectively presented as

$$\widehat{f}(\zeta, \mathbf{W}_n) \triangleq f(\zeta^l, \mathbf{W}_n^l) + \sum_{n\in\mathcal{N}} \mathrm{Tr}\left(\bigtriangledown_{\mathbf{W}_n} f(\zeta^l, \mathbf{W}_n^l)^H (\mathbf{W}_n - \mathbf{W}_n^l)\right) + \bigtriangledown_{\zeta} f(\zeta^l, \mathbf{W}_n^l)(\zeta - \zeta^l), \tag{45a}$$

$$\widehat{f}(\chi_n \rho_n) \triangleq \chi_n^l {\rho_n}^l + \chi_n^l (\rho_n - {\rho_n}^l) + {\rho_n}^l (\chi_n - \chi_n^l). \tag{45b}$$

The problem $\mathbf{P}_{4.2}$ is still non-convex due to the rank-one constraints (43f). Thus, the SDR method is applied. Then, the relaxed problem becomes a convex problem that can be solved by using a standard convex optimization tool, such as CVX [43]. After obtaining $\mathbf{W}_n^{\ddagger}$, $\mathbf{w}_n^{\ddagger}$ can be recovered from $\mathbf{W}_n^{\ddagger} = \mathbf{w}_n^{\ddagger}\mathbf{w}_n^{\ddagger H}$ by applying the eigenvalue decomposition when $\mathrm{Rank}(\mathbf{W}_n^{\ddagger}) = 1$. Otherwise, the suboptimal beamforming vectors can be obtained by using the Gaussian randomization.

D. Phase Shift Optimization

Given any feasible beamforming vectors obtained in the previous subsection, the phase shift optimization problem can be formulated as

$$\mathbf{P}_{4.3}: \max_{\boldsymbol{\Theta},\varsigma,\kappa} \ \eta_{EE}, \tag{46a}$$

$$\text{s.t. s.t. } C2, C3, (6), (16\text{d}), (18\text{b}), (40)-(42), \tag{46b}$$

$$\max_{\substack{\mathbf{h}_{k,I}^H \in \mathcal{H}_{k,I} \\ \mathbf{f}_{k,R} \in \mathcal{F}_{k,R}}} \sum_{n\in N} \left|\mathbf{h}_{k,I}^H \mathbf{w}_n + \mathbf{f}_{k,R}^H \boldsymbol{\Theta} \mathbf{g}_{SI} \mathbf{w}_n\right|^2 \leq p_{tol,k}, \forall k. \tag{46c}$$

Note that both the objective function and constraints are non-convex functions which makes the phase shift design challenging. In order to solve the optimization problem effectively, we first rewrite the quadratic terms in $\mathbf{P}_{4.3}$ by the method adopted in the subsection D of the Section IV. Moreover, the auxiliary variables $\tau_n, Z_n, n \in \mathcal{N}$ are introduced. Furthermore, the SCA is applied to approximate the optimization problem. Then, the phase shift design problem can be rewritten as

$$\mathbf{P}_{4.4}: \max_{\mathbf{E},\boldsymbol{Z},\boldsymbol{\tau},\varsigma,\kappa} \ \frac{1}{P_{tot}} \sum_{n=1}^{N} \log_2(1+\tau_n), \tag{47a}$$

$$\text{s.t. } C2, (18\text{b}), (31\text{d}), (40), (41), \tag{47b}$$

$$\text{Tr}\left(\mathbf{E}\mathbf{v}_n \mathbf{W}_n \mathbf{v}_n^H\right) \geq \widehat{f}(\tau_n Z_n), \forall n, \tag{47c}$$

$$\sum_{i=n+1}^{N} \text{Tr}\left(\mathbf{E}\mathbf{v}_n \mathbf{W}_i \mathbf{v}_n^H\right) + \sum_{k=1}^{K} \text{Tr}\left(\mathbf{E}\mathbf{F}_n\right) p_k^P + n_j \leq Z_n, \forall n, \tag{47d}$$

$$\sum_{n=1}^{N} \text{Tr}\left(\mathbf{E}\bar{\mathbf{H}}_k \mathbf{W}_n \bar{\mathbf{H}}_k^H\right) \leq \kappa_k, \tag{47e}$$

$$\mathbf{E} \succeq 0, \forall n, \tag{47f}$$

$$\text{Rank}\left(\mathbf{E}\right) = 1, \forall n, \tag{47g}$$

where $\widehat{f}(\tau_n Z_n) = \tau_n^l {Z_n}^l + \tau_n^l (Z_n - {Z_n}^l) + {Z_n}^l (\tau - \tau_n^l)$. The problem $\mathbf{P}_{4.4}$ is still non-convex due to the constraint (41) and rank-one constraints. In particular, the constraint (41) contains the quadratic term $\boldsymbol{\Theta} \sum_{n\in N} \mathbf{g}_{SI} \mathbf{W}_n \mathbf{g}_{SI}^H \boldsymbol{\Theta}^H$ which complicates the problem. Thus, by defining $\mathbf{Q} = \sum_{n\in N} \mathbf{g}_{SI} \mathbf{W}_n \mathbf{g}_{SI}^H$, the transformation of constraint (41) can be expressed as

$$\begin{bmatrix} \iota_k \mathbf{I}_M & \mathbf{0} \\ \mathbf{0} & -\iota_k \xi_{k,R}^2 - \kappa_k + \varsigma_k \end{bmatrix} - \mathbf{C}^H \boldsymbol{\Theta} \mathbf{Q} \boldsymbol{\Theta}^H \mathbf{C} \succeq \mathbf{0}, \forall k, \tag{48}$$

where $\mathbf{C} = [\mathbf{I}_M \ \mathbf{0}]$. Then, the eigenvalue decomposition of $\mathbf{Q}$ is $\sum_m \mathbf{u}_m \mathrm{s}_m \mathbf{u}_m^H$, where s_n is the eigenvalue of $\mathbf{Q}$ and the corresponding vectors are denoted by $\mathbf{u}_n$. Thus, constraint (48) can be rewritten as

$$\begin{bmatrix} \iota_k \mathbf{I}_M & \mathbf{0} \\ \mathbf{0} & -\iota_k \xi_{k,R}^2 - \kappa_k + \varsigma_k \end{bmatrix} - \sum_m \mathrm{s}_m \mathbf{D}_m \mathbf{E} \mathbf{G}_m \succeq \mathbf{0}, \forall k, \tag{49}$$

where $\mathbf{D}_m = [\mathbf{C}^H \mathrm{diag}(\mathbf{u}_m) \ \mathbf{0}]$ and $\mathbf{G}_m = \begin{bmatrix} \mathrm{diag}(\mathbf{u}_m^H)\mathbf{C} \\ \mathbf{0} \end{bmatrix}$. Consequently, constraint (49) is a convex function with respect to $\mathbf{E}$. Moreover, by using the SDR method to remove the rank-one constraint, the phase shift design can be expressed as

$$\mathbf{P}_{4.5}: \max_{\mathbf{E}, \boldsymbol{Z}, \boldsymbol{\tau}, \varsigma, \kappa} \ \frac{1}{P_{tot}} \sum_{n=1}^{N} \log_2(1+\tau_n), \tag{50a}$$

$$\text{s.t. } C2, (18\text{b}), (40), (47\text{c}) - (47\text{g}), (49). \tag{50b}$$

Problem $\mathbf{P}_{4.5}$ is a standard SDP problem, which can be solved by using the convex optimization tool [43]. After obtaining $\mathbf{E}^\ddagger$, $\mathbf{e}^\ddagger$ can be given by eigenvalue decomposition if $\mathrm{Rank}(\mathbf{E}^\ddagger) = 1$, otherwise, the approximate $\mathbf{e}$ can be constructed by applying the Gaussian randomization method.

TABLE III

SIMULATION PARAMETERS

Parameters	Notation	Typical Values
Numbers of SUs	N	3
The maximum available transmit power of SBS	$P_{\max}$	25 dBm
The minimum rate threshold of SUs	$R_{\min}$	0.5 Bits/Hz/s
The noise power	σ^2	-110 dBm
The interference tolerance of the kth PU	$p_{tol,k}$	-90 dB
The tolerance error of SCA	ε_{SCA}	10^{-2}
The tolerance error of BCD	ε_{BCD}	10^{-2}
The transmit power of the kth PU	p_k^P	35 dBm
The radiuses of the uncertainty regions	$\xi_{k,I}$, $\xi_{k,R}$	10^{-4}

VI. SIMULATION RESULTS

In this section, simulation results are provided to validate the effectiveness of the proposed algorithms. The simulation settings are based on the works in [15]. The locations of the PBS and SBS are respectively set as $(5, 0, 20)$ and $(5, 100, 20)$. Moreover, the locations of SUs are set as $(5, 165, 0)$, $(5, 145, 0)$ and $(5, 125, 0)$, respectively. The IRS is employed in the secondary network, whose location is set to be

$(0, 125, 2)$. The channels are generated by the model $\mathbf{h}_\beta = \sqrt{G_0(d)^{-c_\beta}}\mathbf{g}_\beta$, where $G_0 = -30$ dB denotes the path loss at the reference point. d denotes the link distance. c_β and $\mathbf{g}_\beta$ denote the path loss exponent and fading component, respectively, where $\beta \in \{D, SI, R\}$. The pass loss exponents for the direct link, SBS-IRS link and IRS-user link are set to be $c_D = 3.5$, $c_{SI} = 2.2$ and $c_R = 2.2$, respectively. The bandwidth is normalized as 1 Hz. The number of channel realizations is 10^3. The detailed simulation settings are given in Table III.

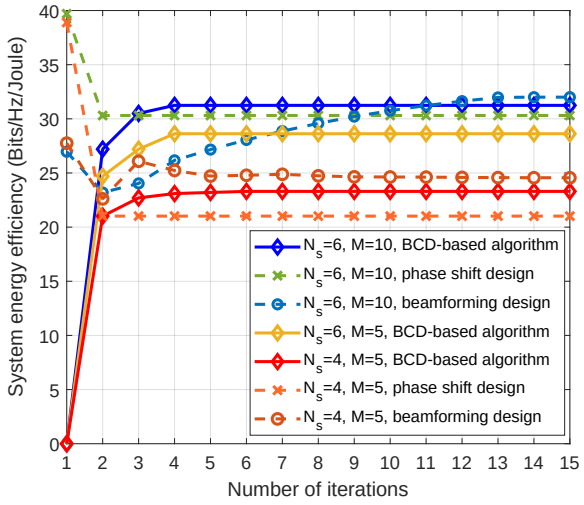

Fig. 2. Convergence of the proposed BCD-based algorithm.

The proposed algorithm under the perfect CSI case is marked as 'BCD-based algorithm', while the imperfect CSI case is marked as 'Robust'. For comparison, four baseline schemes are considered. The first baseline scheme aims to maximize EE, which is marked as 'EE maximization'. The second baseline scheme is the method that with the assistance of IRS, the phase shifts of the IRS are generated randomly, denoted by 'Random phase shifts'. For the third baseline scheme, the IRS reflecting coefficients do not have phase adjustment, which is marked by 'No phase shifts'. The fourth baseline scheme is based on the conventional CRN with NOMA without the assistance of IRS, which is marked as 'No IRS'.

Fig. 2 shows the convergence of the proposed BCD-based algorithm for different numbers of antennas N_s and IRS reflecting elements M. Particularly, three cases are considered: Case 1 with $N_s = 4$ and $M = 5$; Case 2 with $N_s = 6$ and $M = 5$; Case 3 with $N_s = 6$ and $M = 10$. Besides, the convergence of SCA in terms of the beamforming design and IRS phase shift design under Case 1 and Case 3 for the first iteration of the BCD-based algorithm are presented. It is seen that the proposed BCD-based algorithm under all three cases can converge to a stationary point within 5 iterations. For Case 1, both

the beamforming and phase shift design can achieve the saturate value within 10 SCA iterations, while Case 3 needs more iterations for convergence. This is because the solution space is enlarged by the increase of N_s and M. Note that the number of iterations of the proposed BCD-based algorithm is little affected by the number of N_s and M, while the iterations required for SCA are sensitive to the number of antennas and reflecting elements.

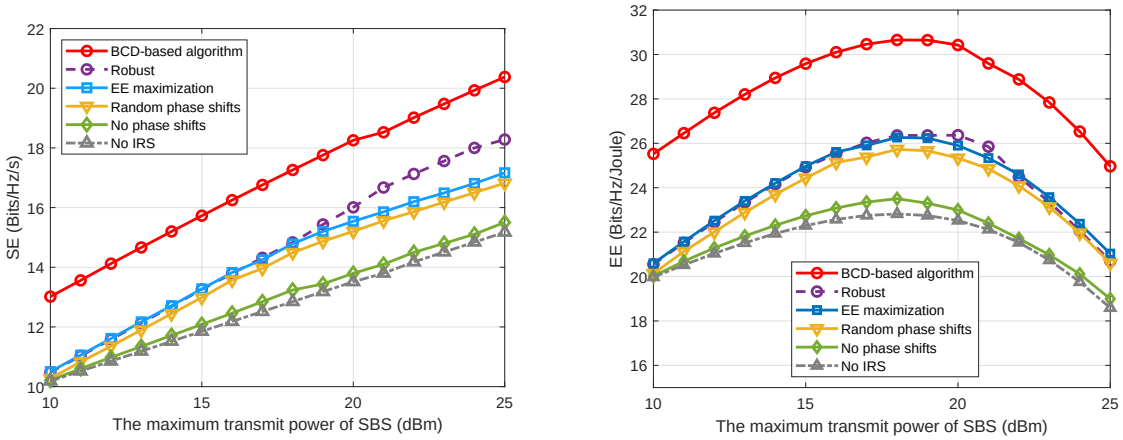

Fig. 3. (a) SE versus the maximum available transmit power; (b) EE versus the maximum available transmit power.

Fig. 3(a) and Fig. 3(b) show the SE and EE versus the SBS maximum available transmit power achieved by different designs, respectively. It is seen from Fig. 3(a) that the proposed BCD-based algorithm under the perfect CSI can achieve the best SE among all schemes. Meanwhile, as shown in Fig. 3(b), the proposed scheme also can achieve a better EE than all baseline schemes. This indicates that the exploitation of IRS in CRNs with NOMA is beneficial for improving both SE and EE. Specifically, in Fig. 3(a), the system SE increases monotonically with the maximum transmit power $P_{\max}$. Moreover, the SE achieved by 'No IRS' baseline scheme is lower than other schemes, which demonstrates that SE can be further improved by the assistance of IRS. As shown in Fig. 3(a), the 'Random phase shifts' and 'No phase shifts' schemes also can achieve better SE performance than those of other baseline scheme without IRS. This indicates that IRS is able to increase the system performance to a certain extent, even without the adjustment of phase shifts. Furthermore, the SE of the proposed method under the imperfect CSI case is similar to that achieved by the 'EE maximization' baseline scheme at the beginning and larger than it with the transmit power increases. The reason is that the MOO framework adopted in this paper can achieve a better balance between SE and EE. Although the SE obtained under the imperfect CSI is lower than that achieved under the perfect CSI owing to the CSI uncertainty, the performance gain in SE still outperforms that of the 'No IRS' baseline scheme. This further manifests that the effectiveness

of the application of IRS in CRNs with NOMA. Besides, the capability of against channel uncertainty of the proposed algorithm is demonstrated. As shown in Fig. 3(b), the achieved EE of all five schemes first increases with the maximum transmit power and then decreases with it. The reason is that, the SBS can utilize more power to serve the SUs when the available transmit power increases. When the transmit power increases a certain value, such as 18 dBm, the increase of SE is slower than the increase speed of power consumption, which results in the decrease of EE. It reveals the tradeoff between EE and SE.

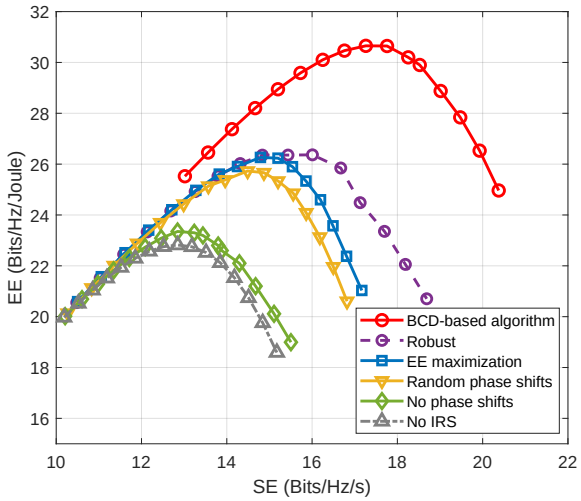

Fig. 4. EE-SE tradeoff for different schemes.

In order to further illustrate the relationship between SE and EE, Fig. 4 shows the tradeoffs between SE and EE of all five schemes in the range of the maximum transmit power constraint from 10dBm to 25dBm. It is seen that the system EE is a quasi-concave function of SE. When SE increases, EE firstly grows and then decreases with it. It indicates that the achievement of higher SE demands more energy consumption. Meanwhile, EE is the ratio of system throughput to energy consumption. When the energy consumption becomes faster than the growth of SE, EE starts to decrease with the increase of SE. Moreover, the tradeoff achieved by the baseline schemes is presented. It is also seen that the proposed BCD-based algorithm can achieve a better SE-EE tradeoff under both the perfect and imperfect CSI cases compared to the other baselines schemes enabled by the joint optimization of SE and EE. It demonstrates that the proposed algorithm has great potential for achieving a superior balance between SE and EE.

Fig. 5 shows the EE of the proposed algorithm versus the number of antennas N_s and IRS elements M. It can be seen that the case with $M = 10, N_s = 6$ can obtain a larger EE than the case with $M = 10, Ns = 4$. It can be explained by the fact that a higher beamforming resolution can be facilitated

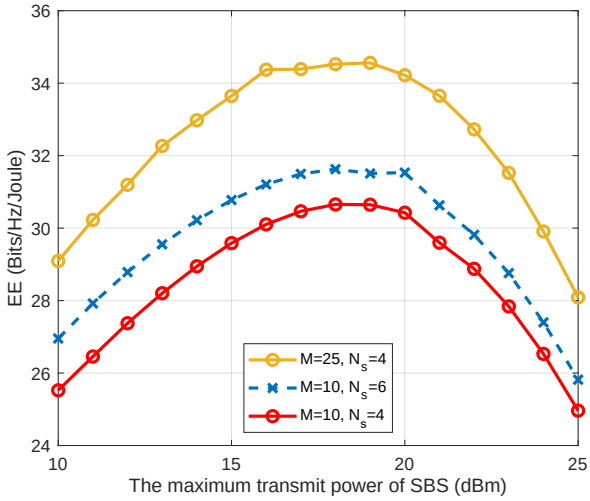

Fig. 5. EE versus the maximum transmit power for different system settings.

by the additional antennas, which leads to a higher SINR. However, the performance achieved by the case with $M = 25, N_s = 4$ is superior to that obtained by the other two cases. The reason is that the transmitted signals of IRS-assisted schemes can obtain a higher power gain at SUs with more IRS elements while the energy consumption remains at a low level due to the passive characteristic of IRS. It is inferred that the deployment of IRS in CRNs with NOMA can achieve the same performance gain as employing additional antennas while the hardware cost is low.

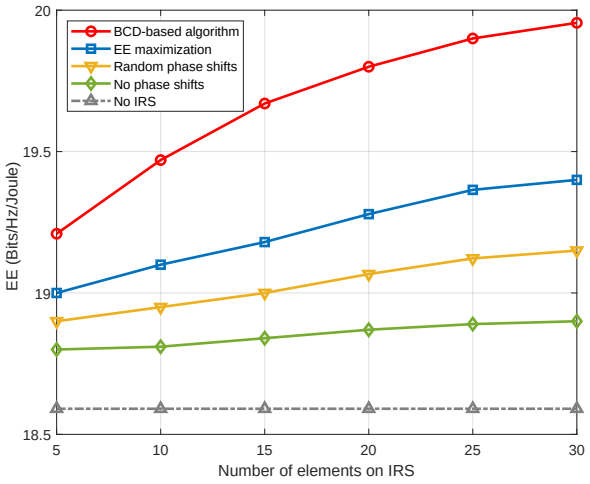

Fig. 6. SE versus the number of elements on IRS.

Fig. 6 shows the impact of the number of IRS elements on the achievable EE of the proposed algorithm and four baseline schemes. It is observed that the EE for all the IRS-assisted schemes increases with M. The EE of the 'No IRS' baseline scheme remains constant with a low value. This is because the transmitted signals of IRS-assisted schemes can obtain a higher power gain at SUs with more IRS elements to assist transmission. Moreover, as shown in Fig. 6, the performance gap between the proposed algorithm and other baseline schemes becomes larger with the increase of the number of IRS elements. This is because as the number of IRS elements increases, a higher power gain can be achieved at SUs. Thus, a smaller energy is consumed to satisfy the achievable rate requirements, which results in the increase of EE. However, the performance gain of the 'Random phase shifts' and 'No phase shifts' baseline schemes is limited since the phase shifts are not optimized.

VII. Conclusion

In this paper, the tradeoff between SE and EE was studied in an IRS-assisted downlink MISO NOMA CRN under both the perfect and imperfect CSI cases. The MOOP framework was formulated by simultaneously maximizing SE and EE via jointly optimizing the beamforming design and the reflection coefficients of IRS. The ϵ-constraint method was adopted to transform the MOOPs into SOOPs. Due to the variables are highly coupled, a BCD-based algorithm was exploited to optimize the beamforming design and IRS reflection coefficients iteratively. In the perfect CSI case, a safe approximation was adopted to transform the intractable maximum interference constraint into a convex constraint. The $\mathcal{S}$-procedure method was capitalized to deal with the channel uncertainty. The proposed BCD-based algorithm was employed for the roust resource allocation design. Simulation results demonstrated that the proposed schemes can achieve a better balance between SE and EE than baseline schemes. Moreover, it is shown that both the SE and EE of the proposed algorithm under the imperfect CSI can still be significantly improved due to the exploitation of IRS.

Appendix A
Proof of Theorem 1

The relaxation of problem $\mathbf{P}_{4.3}$ is jointly convex over all optimization variables. Therefore, the optimal solution is characterized by the KKT conditions. In particular, the Lagrangian function of the relaxation

of problem $\mathbf{P}_{4.3}$ in terms of the beamforming matrix $\mathbf{W}_n$ can be given as

$$\begin{aligned}\mathcal{L} = & a_1\left(\sum_{n=1}^{N}\log_2\left(1+\gamma_n\right)-\widehat{f}(\alpha,\mathbf{W}_n)\right)+a_2\left(\mathrm{Tr}(\mathbf{W}_n\mathbf{v}_n^H\mathbf{e}\mathbf{e}^H\mathbf{v}_n)-\widehat{f}(\gamma_n I_n)\right)\\ & +a_3\left[I_n-\sum_{i=n+1}^{N}\mathrm{Tr}(\mathbf{W}_i\mathbf{v}_n^H\mathbf{e}\mathbf{e}^H\mathbf{v}_n)+|\vartheta_n|^2p_k^P+\sigma^2\right]+a_4\left[P_{\max}-\left(\sum_{n=1}^{N}\mathrm{Tr}\left(\mathbf{W}_n\right)+p_c\right)\right]\\ & +a_5\left[p_{tol,k}-\sum_{n=1}^{N}\mathrm{Tr}\left(\mathbf{W}_n\mathbf{H}_k^H\mathbf{e}\mathbf{e}^H\mathbf{H}_k\right)\right]+a_6\left[\mathrm{Tr}\left(\mathbf{W}_j\mathbf{v}_n^H\mathbf{e}\mathbf{e}^H\mathbf{v}_n\right)-\mathrm{Tr}\left(\mathbf{W}_i\mathbf{v}_n^H\mathbf{e}\mathbf{e}^H\mathbf{v}_n\right)\right]\\ & +\mathrm{Tr}\left(\mathbf{W}_n\mathbf{Y}_n\right)+\boldsymbol{\Upsilon},\end{aligned}\tag{51}$$

where $\boldsymbol{\Upsilon}$ are the terms independent of $\mathbf{W}_n$, $\boldsymbol{a}$ and $\mathbf{Y}_n$ are Lagrange multipliers associated with the corresponding constraints. By checking the KKT conditions with respect to $\mathbf{W}_n$, for the optimal $\mathbf{W}_n^{\ddagger}$, one has

$$\begin{aligned}&\boldsymbol{a}^{\ddagger}\geq 0,\ \ \mathbf{Y}_n\succeq 0,\\ &\mathbf{Y}_n^{\ddagger}\mathbf{W}_n^{\ddagger}=0,\ \ \bigtriangledown_{\mathbf{W}_n^{\ddagger}}\mathcal{L}=0,\end{aligned}\tag{52}$$

where $\boldsymbol{a}^{\ddagger}$ and $\mathbf{Y}_n^{\ddagger}$ are the optimal Lagrange multipliers while the $\bigtriangledown_{\mathbf{W}_n^{\ddagger}}\mathcal{L}$ represents the gradient vector of $\mathcal{L}$ with respect to $\mathbf{W}_n^{\ddagger}$. The $\bigtriangledown_{\mathbf{W}_n^{\ddagger}}\mathcal{L}$ is explicitly expressed as

$$\mathbf{Y}_n^{\ddagger}=a_4\mathbf{I}_{N_s}+\boldsymbol{\Delta}_n^{\ddagger},\tag{53}$$

where $\boldsymbol{\Delta}_n^{\ddagger}$ is given by $a_1\bigtriangledown_{\mathbf{W}_n}\hat{f}(\mathbf{W}_n^{\ddagger})-(a_2+a_6)\,\mathbf{v}_n^H\mathbf{e}\mathbf{e}^H\mathbf{v}_n+a_5\mathbf{H}_k^H\mathbf{e}\mathbf{e}^H\mathbf{H}_k$.

Then, we will prove the optimal beamforming matrix $\mathbf{W}_n^{\ddagger}$ is rank-one by unveiling the structure of matrix $\mathbf{Y}_n^{\ddagger}$. The maximum eigenvalue of matrix $\boldsymbol{\Delta}_n^{\ddagger}$ is denoted by $\nu_{max}\in\mathbb{R}$. Note that due to the randomness of the channels, the probability of the case where multiple eigenvalues have the same value $\nu_{max}\in\mathbb{R}$ is zero. According to (54), if $\nu_{max}>a_4$, $\mathbf{Y}_n^{\ddagger}$ cannot be positive semidefinite which contradicts $\mathbf{Y}_n\succeq 0$. On the other hand, if $\nu_{max}\leq a_4$, $\mathbf{Y}_n^{\ddagger}$ is positive semidefinite with $\mathrm{Rank}(\mathbf{Y}_n^{\ddagger})\geq N_s-1$. According to $\mathbf{Y}_n^{*}\mathbf{W}_n^{\ddagger}=0$, $\mathrm{Rank}(\mathbf{W}_n^{\ddagger})=1$. The proof is completed.

REFERENCES

[1] S. Dang, O. Amin, B. Shihada, and M.-S. Alouini, "What should 6G be?," *Nat. Electron.*, vol. 3, pp. 20-29, Jan. 2020.

[2] Q. Wu, T. Ruan, F. Zhou, Y. Huang, F. Xu, S. Zhao, Y. Liu, and X. Huang, "A unified cognitive learning framework for adapting to dynamic environment and tasks," *IEEE Wireless Commun.*, to be published, 2021.

[3] L. Dai, B. Wang, Y. Yuan, S. Han, I. Chih-lin and Z. Wang, "Non-orthogonal multiple access for 5G: solutions, challenges, opportunities, and future research trends," *IEEE Commun. Mag.,* vol. 53, no. 9, pp. 74-81, Sep. 2015.

[4] Z. Ding, X. Lei, G. K. Karagiannidis, R. Schober, J. Yuan and V. K. Bhargava, "A survey on non-orthogonal multiple access for 5G networks: Research challenges and future trends," *IEEE J. Sel. Areas Commun.,* vol. 35, no. 10, pp. 2181-2195, Oct. 2017.

[5] Y. Liu, Z. Qin, M. Elkashlan, Z. Ding, A. Nallanathan, and L. Hanzo, "Nonorthogonal multiple access for 5G and beyond," *Proc. IEEE,* vol. 105, no. 12, pp. 2347-2381, Dec. 2017.

[6] F. Zhou, Y. Wu, Y. Liang, Z. Li, Y. Wang and K. Wong, "State of the art, taxonomy, and open issues on cognitive radio networks with NOMA," *IEEE Wireless Commun.,* vol. 25, no. 2, pp. 100-108, April 2018.

[7] F. Zhou, Z. Chu, H. Sun, R. Q. Hu, and L. Hanzo, "Artificial noise aided secure cognitive beamforming for cooperative MISO-NOMA using SWIPT," *IEEE J. Sel. Areas Commun.,* vol. 36, no. 4, pp. 918-931, April 2018.

[8] L. Lv, J. Chen, Q. Ni, Z. Ding and H. Jiang, "Cognitive non-orthogonal multiple access with cooperative relaying: A new wireless frontier for 5G spectrum sharing," *IEEE Commun. Mag.,* vol. 56, no. 4, pp. 188-195, April 2018.

[9] Z. Ding, Y. Liu, J. Choi et al., "Application of non-orthogonal multiple access in LTE and 5G networks," *IEEE Commun. Mag.,* vol. 55, no. 2, pp. 185-191, Feb. 2017.

[10] L. Lv, J. Chen, Q. Li, and Z. Ding, "Design of cooperative nonorthogonal multicast cognitive multiple access for 5G systems: User scheduling and performance analysis," *IEEE Trans. Commun.,* vol. 65, no. 6, pp. 2641-2656, Jun. 2017.

[11] Q. Wu and R. Zhang, "Towards smart and reconfigurable environment: Intelligent reflecting surface aided wireless network," *IEEE Commun. Mag.,* vol. 58, no. 1, pp. 106-112, Jan. 2020.

[12] Q. Wu and R. Zhang, "Intelligent reflecting surface enhanced wireless network via joint active and passive beamforming," *IEEE Trans. Wireless Commun.,* vol. 18, no. 11, pp. 5394-5409, Nov. 2019.

[13] S. Abeywickrama, R. Zhang, Q. Wu and C. Yuen, "Intelligent reflecting surface: Practical phase shift model and beamforming optimization," *IEEE Trans. Commun.,* vol. 68, no. 9, pp. 5849-5863, Sept. 2020.

[14] Q. Wu and R. Zhang, "Joint active and passive beamforming optimization for intelligent reflecting surface assisted SWIPT under QoS constraints," *IEEE J. Sel. Areas Commun.,* vol. 38, no. 8, pp. 1735-1748, Aug. 2020.

[15] Q. Wang, F. Zhou, R. Q. Hu, an Y. Qian, "Energy efficient robust beamforming and cooperative jamming design for IRS-assisted MISO networks," *IEEE Trans. Wireless Commun.,* vol. 20, no. 4, pp. 2592-2607, Apr. 2021.

[16] F. Fang, H. Zhang, J. Cheng and V. C. M. Leung, "Energy-Efficient Resource Allocation for Downlink Non-Orthogonal Multiple Access Network," *IEEE Trans. Commun.,* vol. 64, no. 9, pp. 3722-3732, Sept. 2016.

[17] F. Fang, H. Zhang, J. Cheng, S. Roy and V. C. M. Leung, "Joint user scheduling and power allocation optimization for energy-efficient NOMA systems with imperfect CSI," *IEEE J. Sel. Areas Commun.,* vol. 35, no. 12, pp. 2874-2885, Dec. 2017.

[18] M. F. Hanif, Z. Ding, T. Ratnarajah and G. K. Karagiannidis, "A minorization-maximization method for optimizing sum rate in the downlink of non-orthogonal multiple access systems," *IEEE Trans. Signal Process.,* vol. 64, no. 1, pp. 76-88, Jan. 2016.

[19] Q. N. Le, A. Yadav, N. -P. Nguyen, O. A. Dobre and R. Zhao, "Full-duplex non-orthogonal multiple access cooperative overlay spectrum-sharing networks with SWIPT," *IEEE Trans. Green Commun. and Netw.,* vol. 5, no. 1, pp. 322-334, Mar. 2021.

[20] Z. Ding, R. Schober and H. Vincent Poor, "No-pain no-gain: DRL assisted optimization in energy-constrained CR-NOMA networks," *IEEE Trans. Commun.,* to be published, 2021.

[21] D. Xu and H. Zhu, "Sum-Rate Maximization of Wireless Powered Primary Users for Cooperative CRNs: NOMA or TDMA at Cognitive Users?," *IEEE Trans Commun.,* vol. 69, no. 7, pp. 4862-4876, July 2021.

[22] Y. Zhang, Q. Yang, T.-X. Zheng, H.-M. Wang, Y. Ju, and Y. Meng, "Energy efficiency optimization in cognitive radio inspired non-orthogonal multiple access," *Proc. IEEE 27th PIMRC,* pp. 1-6, Sep. 2016.

[23] H. Sun, F. Zhou, and Z. Zhang, "Robust beamforming design in a NOMA cognitive radio network relying on SWIPT," *Proc. IEEE Int. Cof. Commun. (ICC)*, Kansas City, USA, pp. 1-6, Jul. 2018.

[24] H. Sun, F. Zhou, R. Q. Hu, and L. Hanzo, "Robust beamforming design in a NOMA cognitive radio network relying on SWIPT," *IEEE J. Sel. Areas Commun.,* vol. 37, no. 1, pp. 142-155, Jan. 2019.

[25] M. Zeng, X. Li, G. Li, W. Hao and O. A. Dobre, "Sum rate maximization for IRS-assisted uplink NOMA," *IEEE Commun. Lett.,* vol. 25, no. 1, pp. 234-238, Jan. 2021.

[26] X. Mu, Y. Liu, L. Guo, J. Lin, and N. Al-Dhahir, "Exploiting intelligent reflecting surfaces in NOMA networks: Joint beamforming optimization," *IEEE Trans. Wireless Commun.,* vol. 19, no. 10, pp. 6884-6898, Oct. 2020.

[27] Z. Zhang, L. Lv, Q. Wu, H. Deng, and J. Chen, "Robust and secure communications in intelligent reflecting surface assisted NOMA networks," *IEEE Commun. Lett.,* vol. 25, no. 3, pp. 739-743, Mar. 2021.

[28] G. Yang, X. Xu, and Y.-C. Liang, "Intelligent reflecting surface assisted non-orthogonal multiple access," *Proc. IEEE Wireless Commun. and Netw. Conf. (WCNC)*, pp. 1-6, May 2020.

[29] G. Yang, X. Xu, Y.-C. Liang, and M. D. Renzo, "Reconfigurable intelligent surface-assisted non-orthogonal multiple access," *IEEE Trans. Wireless Commun.,* vol. 20, no. 5, pp. 3137-3151, May 2021.

[30] W. Ni, X. Liu, Y. Liu, H. Tian, and Y. Chen, "Resource allocation for multi-cell IRS-aided NOMA networks," *IEEE Trans. Wireless Commun.,* vol. 20, no. 7, pp. 4253-4268, Feb. 2021.

[31] F. Fang, Y. Xu, Q.-V. Pham, and Z. Ding, "Energy-efficient design of IRS-NOMA networks," *IEEE Trans. Veh. Tech.,* vol. 69, no. 11, Nov. 2020.

[32] M. Fu, Y. Zhou, Y. Shi, and K. B. Letaief, "Reconfigurable intelligent surface empowered downlink non-orthogonal multiple access," *IEEE Trans. Commun.,* vol. 69, no. 6, Jun. 2021.

[33] X. Liu, Y. Liu, Y. Chen and H. V. Poor, "RIS enhanced massive non-orthogonal multiple access networks: Deployment and passive beamforming design," *IEEE J. Sel. Areas Commun.,* vol. 39, no. 4, pp. 1057-1071, Apr. 2021.

[34] X. Guan, Q. Wu, and R. Zhang, "Joint power control and passive beamforming in IRS-assisted spectrum sharing," *IEEE Commun. Lett.*, vol. 24, no. 7, pp. 1553-1557, Jul. 2020.

[35] D. Xu, X. Yu, and R. Schober, "Resource allocation for intelligent reflecting surface-assisted cognitive radio networks," *Proc. IEEE 20th Int. Workshop Signal Process. Adv. Wireless Commun. (SPAWC)*, pp. 1-5, May, 2020.

[36] D. Xu, X. Yu, Y. Sun, D. W. K. Ng, and R. Schober, "Resource allocation for IRS-assisted full-duplex cognitive radio systems," *IEEE Tran. Commun.*, vol. 68, no. 12, pp. 7376-7394, Dec. 2020.

[37] J. Tang, D. K. So, E. Alsusa, and K. A. Hamdi, "Resource efficiency: A new paradigm on energy efficiency and spectral efficiency tradeoff," *IEEE Trans. Wireless Commun.,* vol. 13, no. 8, pp. 4656-4669, Aug. 2014.

[38] S. Zarandi, A. Khalili, M. Rasti, and H. Tabassum, "Multi-objective energy efficient resource allocation and user association for in-band full duplex small-cells," *IEEE Trans. Green Commun. and Netw.,* vol. 4, no. 4, pp. 1048-1060, Dec. 2020.

[39] J. Wang and D. P. Palomar, "Worst-case robust MIMO transmission with imperfect channel knowledge," *IEEE Trans. Signal Process.*, vol. 57, no. 8, pp. 3086-3100, Aug. 2009.

[40] K. Chircop and D. Zammit-Mangion, "On epsilon-constraint based methods for the generation of Pareto frontiers," *J. Mech. Eng. Autom.,* vol. 3, pp. 279-289, May 2013.

[41] S. Zarandi, A. Khalili, M. Rasti, and H. Tabassum, "Multi-objective energy efficient resource allocation and user association for in-band full duplex small-cells," *IEEE Trans. Green Commun. and Netw.,* vol. 4, no. 4, pp. 1048-1060, Dec. 2020.

[42] Q. Li, M. Hong, H.-T. Wai, Y.-F. Liu, W.-K. Ma, and Z.-Q. Luo, "Transmit solutions for MIMO wiretap channels using alternating optimization," *IEEE J. Sel. Areas Commun.,* vol. 31, no. 9, pp. 1714-1727, Sep. 2013.

[43] M. Grant and S. Boyd, "CVX: Matlab software for disciplined convex programming, version 2.1," 2014.

[44] S. P. Boyd and L. Vandenberghe, *Convex Optimization.* Cambridge, U.K.: Cambridge Univ. Press, 2004.